RAW 264.7 MACROPHAGE-MEDIATED DEPLETION OF HYDROGEN PEROXIDE
IN CELL CULTURE MEDIA

by

DIMITRIOS NESTOR KARASTATHIS

DDS., The University of Toronto, 2006

A THESIS SUBMITTED IN PARTIAL FULFILLMENT OF THE REQUIREMENTS FOR
THE DEGREE OF

MASTER OF SCIENCE

in

THE FACULTY OF GRADUATE STUDIES

(Craniofacial Science)

THE UNIVERSITY OF BRITISH COLUMBIA

(Vancouver)

February 2011

Abstract

Macrophages are known to produce hydrogen peroxide that act both as part of the host defense system, and as secondary messenger. As hydrogen peroxide has powerful effects and macrophages, which are found at rough implant surfaces, must function in an environment containing it, it is of interest to know how hydrogen peroxide levels are regulated. The current study was conducted in order to determine whether RAW 264.7 macrophages were capable of depleting exogenously added hydrogen peroxide.

Conditions for optimal detection of H_2O_2 using Amplex Red fluorescence were investigated under a variety of conditions. The ability of RAW 264.7 cells to produce and/or deplete extracellular hydrogen peroxide was determined when cell concentrations, times and incubation temperatures were varied. Other possible influences were also examined, including passages of cells in culture, H_2O_2 stimulation with LPS, and catalase inhibition via 3AT.

Using Amplex Red to detect hydrogen peroxide, it was found that PBS and black welled microplates provided the most reliable conditions for detection. In addition, direct contact of Amplex Red with RAW 264.7 macrophages was found to interfere with the detection reagent's ability to detect exogenous hydrogen peroxide. Most importantly, RAW 264.7 macrophages were found to deplete exogenous hydrogen peroxide, regardless of any previously treatment with LPS. This depletion was found to be time, cell concentration, temperature and passage number dependent. The use of a catalase inhibitor, 3AT, had no effect on reducing the ability of RAW 264.7 cells to deplete hydrogen peroxide from its surrounding environment, and was also found to lower the detection capacity of Amplex Red.

The measurement of H_2O_2 produced by RAW 264.7 macrophages is difficult to determine, as our results using a specific H_2O_2 detection reagent demonstrated that the macrophages depleted any H_2O_2 in the media. The manner of depletion was found to be time, cell concentration, temperature, and passage number dependent. The anticipated stimulating effect of LPS was not observed, and the anticipated inhibitory effect of 3AT could not be detected, suggesting that macrophage depletion of exogenous hydrogen peroxide did not involve catalase.

Table of Contents

List of Tables

List of Figures

List of Abbreviations

AGT: O^6-alkylguanine-DNA alkyltransferase
AP-1: Activator Protein-1
APC: Antigen Presenting Cell
ATCC: American Type Culture Cell
BALB: Bagg Albino
CAT: Chloramphenicol Acetyltransferase
Cu^+: Cuprous Copper
CuZnSOD: Copper-Zinc-Superoxide Dismutase
DCFDA: 2',7'-dichlorodihydrofluorescein diacetate
DNA: Deoxyribonucleic Acid
DNFB: 2,4-dinitrofluorobenzne
ECSOD: Extracellular Superoxide Dismutase
Fe^{2+}: Ferrous Iron
Fe^{3+}: Ferric Iron
Flt-1: fms-Related Tyrosine Kinase 1
GPx: Glutathione Peroxidase
GRD: Glutathione Reductase
GSH: γ-glutamylcysteinylglycine
GSSG: Glutathione Disulfide
H_2O_2: Hydrogen Peroxide
HeLa: Henrietta Lacks Cell Line
HRP: Horse Radish Peroxidase
IFN-γ: Interferon - gamma
IL-1α: Interleukin-1 alpha
IL-1 β: Interleukin-1 beta
IL-6: Interleukin-6
iNOS: Inducible Nitric Oxide Synthase
LPS: Lipopolysaccharide
M1: Classically Activated Macrophage
M2: Alternatively Activated Macrophage
MAP: Mitogen-Activated Protein
MCP-1: Monocyte Chemotactic Protein-1
MHC: Major Histocompatibility Complex
MMP: Matrix Metalloproteinase
MnSOD: Manganese Superoxide Dismutase
mRNA: Messenger Ribonucleic Acid
MuLV: Murine Leukemia Virus
NAC: N-acetyl cysteine
NADPH: Nicotinamide Adenine Dinucleotide Phosphate
NF-kB: Nuclear Factor-Kappa beta
NO: Nitric Oxide
O_2: Oxygen

$O_2^{\bullet-}$: Superoxide Anion
OH•: Hydroxyl Radical
$OONO^-$: Peroxynitrite
OX: Oxidized
PC1: Monoboronated Resorufin
PDTC: Pyrollidine Dithiocarbamate
PG1: Monoboronated 2-methyl-4-methoxy Tokyo Green
PMA: Phorbol 12-myristate 13-acetate
Prx: Peroxiredoxins
PTPase: Protein Tyrosine Phosphatases
Red: Reduced
ROS: Reactive Oxygen Species
SOD: Superoxide Dismutase
SRBC: Sheep Red Blood Cell
TGF-β: Transforming Growth Factor-beta
Th2: T Helper-type 2
TMB: 3, 5, 3', 5'-Tetramethylbenzidine
TNF-α: Tumor Necrosis Factor-alpha
TNF-β: Tumor Necrosis Factor-beta
VEGF: Vascular Endothelial Growth Factor
XO: Xylenol Orange

Acknowledgements

I would personally like to thank Drs. Brunette, Waterfield and Putnins for their direction, wisdom and most importantly patience, during this entire thesis process. Without them, my thirst for knowledge would have been quenched years ago.

In addition, there are numerous individuals that have helped me over the last three years that cannot go unmentioned. I would like to thank Jim Firth who was always willing to provide a helping hand, no matter how busy he was; Salem the encyclopedia of macrophages; Fumiko and Hazel who were the best lab techs anyone could ask for; Katrin the chemistry wizard; Vince my poster nemeses; Jolanda the stats queen; the unknown UBC janitor who occasionally let me into the lab when I would lock myself out at night; and the little knight at the side of my desk, whose battle hardened axe was always ready to strike, if I ever fell asleep writing this thesis.

Dedication

This thesis is dedicated to the three most important people in my life:

To my mother and father, who since I was little, have always supported me in whatever I did. It is thanks to them and their ever-lasting love that I have achieved all my goals. This is only but a small tribute to all they have sacrificed for me.

To Devon, the love of my life. Were it not for her patience, wisdom and love, I would never have finished this project. You are the light that has guided this lost traveler through the darkness.

1 Review of the Literature

1.1 Wound Healing

1.1.1 Introduction

Normal wound healing involves a complex interaction among various cell types, cytokines, growth factors and extracellular matrix (Watkins et al., 2008), and is commonly divided into three sequential phases: inflammation (early and late), granulation tissue formation, and matrix formation and remodeling (Wikesjo et al., 1999) (figure 1). The inflammation phase begins immediately upon injury and lasts for about 10 days; the granulatory phase begins days after injury and lasts for 3-4 weeks; and the remodeling phase begins weeks after injury and lasts for 3-4 months (Watkins et al., 2008). It is important to note that stages may overlap considerably and the time needed for completion of each stage may vary, depending on local and systemic factors (Polimeni 2006).

1.1.2 Phases of Wound Healing

1.1.2.1 Inflammation Phase

Upon traumatic injury to a tissue, the inflammatory phase initiates with vasodilation, allowing fluid to leak into the extravascular space. Platelets are recruited to the wound to stop blood loss (Watkins et al., 2008) and within seconds plasma proteins, primarily fibrinogen, precipitate onto the wound surfaces and provide an initial basis for adherence of a fibrin clot (Wikesjo et al., 1999). The clot has two functions: it temporarily protects the denuded tissues, and serves as a provisional matrix for cell migration (Polimeni et al., 2006). Within the first hour, neutrophils begin infiltrating into the surrounding area. The role of the neutrophil includes removal of injured and necrotic tissue (Wikesjo et al., 1999), along with cleansing the wound of bacteria through phagocytosis and release of enzymes and toxic oxygen products (Polimeni et al., 2006). Within 3 days, the inflammatory reaction moves into its late phase. Macrophages migrate into the wound area and perform numerous functions including wound debridement (removing old blood cells, neutrophils, and residual tissue debris), secretion of polypeptide mediators (Polimeni

et al., 2006), and antigen presentation to T helper cells (CD4+). The presentation of an antigen to a T helper cell leads to the production of cytokines which activates: additional macrophages to produce IL-1 and TNF; B cells to produce antibodies and memory cells; and cytotoxic T cells (CD8+) which kill virus infected or tumor cells (Robbins et al., 2003; and Vander et al., 2001).

1.1.2.2 Granulation Tissue Formation Phase

This second phase creates the framework necessary for the production of a new functional barrier. Neovascularization of a *de novo* vascular network, and fibroplasia (Watkins et al., 2008) are key elements to the creation of granulation tissue within the wound. The principal cell type involved in this stage is the myofibroblast (Watkins et al., 2008), but macrophages are also involved as they secrete growth factors and cytokines regulating the proliferation and migration of fibroblasts, endothelial cells and smooth muscle cells into the wound area (Polimeni et al., 2006) (figure 2).

1.1.2.3 Matrix Remodeling Phase

After about seven days, the phase of granulation tissue formation gradually enters into the third phase of wound healing, in which the newly formed cell-rich tissue undergoes maturation and remodeling to meet functional demands (Wikesjo et al., 1999). Most of the cells and extracellular matrix materials, such as collagen and elastin, are reorganized or destroyed in an attempt to recreate a prewound state (eg. Collagen is remodeled from type III to prewound type I) (Watkins et al., 2008). Maturation of the granulation tissue results in either the regeneration of the original structures, or repair (scar formation) of the injured tissues (Polimeni et al., 2006).

Figure 1: Phases of Wound Repair
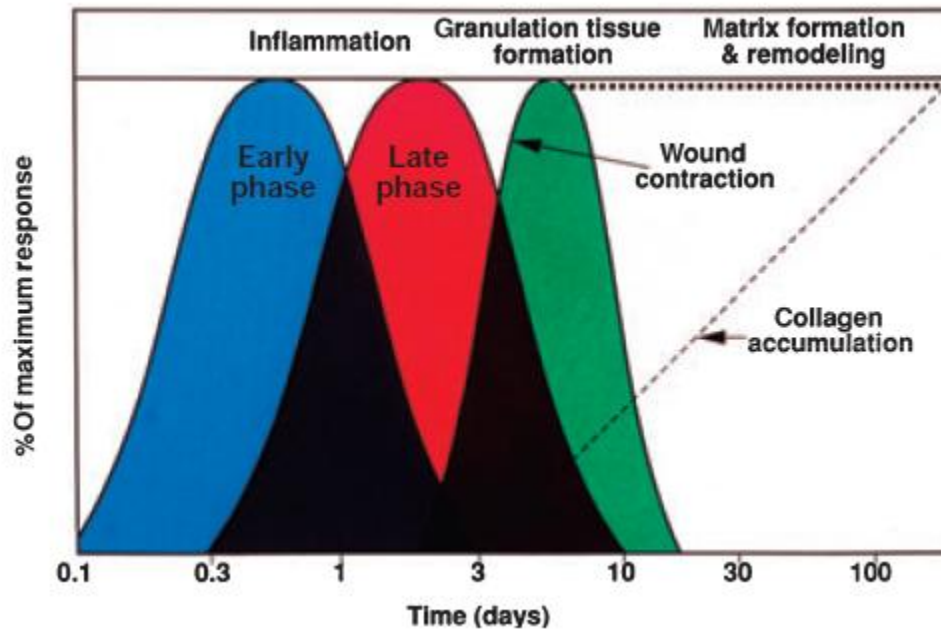
Figure 2: Time Course of Different Cells Appearing in the Wound During the Healing Process
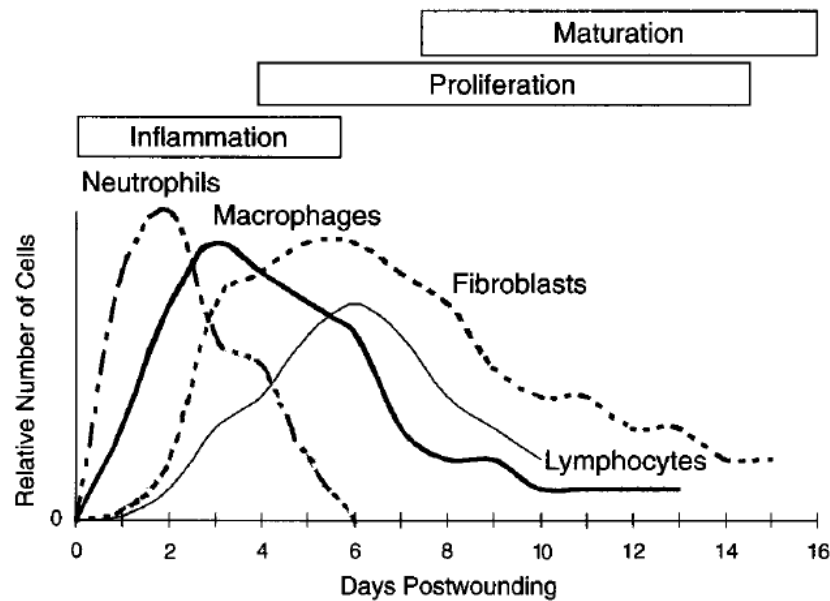
Macrophages and neutrophils are predominant during inflammation, whereas lymphocytes peak somewhat later and fibroblasts are predominant during the proliferative phase

The basic mechanisms, including macrophage participation, and timelines seen in normal wound healing are also observed after placement of oral implants.

1.1.3 Implant Healing

In general, the basic principles of wound healing also apply to implanted devices. However, there are certain wound healing characteristics unique to implants. Experiments performed with titanium implants inserted into the tibias of rabbits demonstrated that at day 1 a large number of biconcave erythrocytes in a network of fibrin is formed at the interface of the bone and implant cavity. At 3 days, red blood cells and scattered macrophages, often enmeshed in a fibrin network, predominate at the implant surface. At 7 days, osteoblasts and osteoclasts are detected at the surface of the bone surrounding the implant, whereas multicellular giant cells are found adhering to the implant surface. Isolated fragments of bone from the surgical procedure are surrounded by macrophages, which also contain sections of bone mineral within their phagocytic vacuoles. In addition, mesenchymal cells begin to appear in the endosteum-implant region. After 14 days, densely packed mesenchymal cells are present close to the implant surface and begin to form a collagenous matrix that is gradually mineralized. Numerous basic multicellular units (organized structures of groups of osteoclasts and osteoblasts together with blood vessels) begin appearing in the cortical bone surrounding the implant. A comparable picture is observed 4 weeks after wounding (Sennerby et al., 1994; Slaets et al., 2006).

As seen above, wound and implant healing is made up of a number of complex mechanisms, in which the macrophage plays a substantial role.

1.2 The Role of the Macrophage

1.2.1 Introduction

The macrophage plays numerous important roles in carrying out its host defense mission. Originating as a monocyte travelling within the circulatory system, the cell migrates into tissues where it develops into a macrophage under the influence of adhesion molecules and chemotactic

factors (Robbins et al., 2003). Some macrophages continue to migrate throughout the body, while others reside permanently in certain tissues: in lung (alveolar macrophage), liver (Kupffer's cells), kidney (mesangial cells), brain (microglial cells) and connective tissues (histiocytes) (Campbell et al., 1999). Important functions of the macrophage include: phagocytosis; acting as an antigen presenting cell (APC); and production of cytokines and reactive oxygen species.

1.2.2   Phagocytosis

Phagocytosis occurs when a microbe presents certain recognizable molecules on its cell surface like antibodies, complement, and/or surface oligosaccharides (Alberts et al., 2008). These surface molecules interact with pattern recognition receptors on the macrophage outer membrane, leading to a conformational change in macrophage cytoskeleton and creation of pseudopodia. The pseudopodia extend around the selected cell and engulf it within the outer membrane of the macrophage. This structure, known as a phagosome, pinches off from the existing macrophage outer membrane, and moves within the cell where its contents are digested.

1.2.3   Antigen Presentation

Ingested and degradative tissue products can be used by the macrophage to activate the adaptive immune response. Newly internalized fragments are bound to macrophage synthesized class I and II major histocompatibility complex (MHC) proteins, which are then transported to the cell surface for display on the plasma membrane (Vander et al., 2001). The macrophage can then present its antigen (antigen presenting cell) to other cells, like T Helper cells, which bind to the fragment-MHC complex and commence other immune processes, such as the adaptive immune response.

1.2.4   Cytokine Release

The interaction of macrophages with stimuli such as interferon-γ (IFN-γ) and lipopolysaccharide (LPS), leads to a phenotypic change into what is known as the classically activated macrophage (M1). This macrophage is characterized by the expression of proinflammatory cytokines such as IL-1α and β, TNF-α, IL-6, IL-12, IL-18 and matrix metalloproteinases (Fairweather et al., 2009;

and De Nardin, 2001), which have all been demonstrated to lead to further inflammation and destruction of bacteria, viruses and host tissues (Van Dyke 2007; Southerland et al., 2006; Dennison et al., 1997). Stimulation of macrophages with IL-4, IL-13, IL-10, transforming growth factor beta (TGF-β), glucocorticoids, immune complexes, LPS and/or IL-1β can transform the cell into the alternatively activated macrophage (M2) (Fairweather et al., 2009). This cell is associated with the release of cytokines such as TGF-β and IL-10, and is linked to Th2 responses, elimination of helminth infections, and wound healing following tissue damage (Fairweather et al., 2009).

1.2.5   Reactive Oxygen Species Production (the respiratory burst)

Another consequence of the ingestion of bacteria is the production of a respiratory burst. As mentioned above, when a microbe is phagocytosed into a macrophage, it is encased in a phagosome. In order to further process its contents, the phagosome may combine with a lysosome to form a phagolysosome, within which microbes are killed by the production of reactive oxygen species (ROS), nitrogen intermediates, and proteolytic enzymes.

1.2.5.1   Reactive Oxygen Species

The production of ROS like superoxide anion, hydroxyl radical and hydrogen peroxide is known as respiratory burst, and is controlled primarily by the phagocyte oxidase system. Phagocyte oxidase is a multisubunit enzyme that is assembled in the phagolysosomal membrane. This enzyme specifically reduces molecular oxygen into ROS, with nicotinamide adenine dinucleotide phosphate (NADPH) acting as a cofactor.

1.2.5.2   Reactive Nitrogen Intermediates

Reactive nitrogen intermediates, mainly nitric oxide (NO), also aid in destroying ingested microbes by combining with hydrogen peroxide or superoxide to produce highly reactive peroxynitrite radicals. The production of NO is aided by the action of inducible nitric oxide synthase (iNOS). This enzyme catalyzes the conversion of arginine to citrulline, and freely diffusible nitric oxide gas is released (Abbas et al., 2007).

Of note is that the extracellular release of ROS, nitrogen intermediates, and/or proteolytic enzymes from macrophages can not only lead to the destruction of extracellular foreign microbes, but may also disrupt surrounding host tissues.

1.2.6   RAW 264.7 Macrophage Cell Line

Although the American Type Culture Cell (ATCC) company catalog supplies up to 23 different macrophage cell lines for research purposes (ATCC Cell Line Index Catalog), the murine macrophage-like cell line RAW 264.7 is the most commonly used mouse macrophage cell line in medical research (Hartley et al., 2008). The cell line was derived some 30 years ago from a tumor developing in a BALB/14 mouse (a BALB/c IgH congenic strain) inoculated with the Abelson murine leukemia virus (MuLV), and replication-competent Moloney helper virus (Mo-MuLV) (Hartley et al., 2008). The RAW 264.7 macrophage has been documented to have properties of normal macrophages including the ability to pinocytose neutral red, phagocytose zymosan and latex beads, lyse antibody-coated SRBC targets and secrete lysozyme (Raschke et al., 1978). RAW 264.7 cells are capable of growing in a base medium of Dulbecco's Modified Eagle's Medium, are adherent to surfaces (ATCC Product Information Sheet), and demonstrate growth inhibition in the presence of sub-ng/ml quantities of lipopolysaccharide (Raschke et al., 1978). The RAW 264.7 macrophage was utilized in this study, as it is a well characterized cell line that is used extensively, and thus results can be readily compared to those obtained in other laboratories.

In order to measure intracellular concentrations of ROS, Kimura et al (2008) treated RAW 264.7 cells with 100µg/ml LPS and found that ROS production peaked after 12-24 hours of LPS stimulation relative to controls. In contrast, ROS production was inhibited by pretreatment of RAW 264.7 cells with N-acetyl cysteine (NAC). All measurements of ROS levels were conducted using 2',7'-dichlorodihydrofluorescein diacetate (DCFDA). In a similar study, Yoo et al (2002) treated RAW 264.7 cells with 5ng/ml IL-1β for 0-60 minutes and demonstrated an increased production of ROS relative to control, as seen via DCFDA and confocal laser scanning fluorescence microscopy. Pretreatment of cells with N-acetyl cysteine (NAC) almost completely inhibited ROS production. Similar results were also found by Kim et al (2009), who

demonstrated increases in ROS production when RAW 264.7 cells were treated with 2,4-dinitrofluorobenzne (DNFB), as measured by DCFDA.

Other investigators have attempted to investigate the release of specific ROS such as hydrogen peroxide. Park et al (1999) cultured RAW 264.7 cells with and without 20ng/ml LPS for 24 hours. Results after 24 hours using DCFDA indicated that 15nM of H_2O_2 was generated by cells without LPS treatment, whereas those treated with LPS produced 25nM. In another study by Woo et al (2004), RAW 264.7 cells were incubated with DCFDA for 30 minutes, before being treated with 100ng/ml LPS for another half hour. The treatment resulted in a 50% increase in DCFDA fluorescence relative to an untreated control. In an experiment which specifically examined the extracellular production of H_2O_2 using Amplex Red, Mantena et al (2008) treated Raw 264.7 cells with S. Typhimurium SL1344 and *pur*G mutant, and found increased amounts of H_2O_2 production over 10 hours. H_2O_2 production specific to SL1344 was inhibited by the ROS inhibitors suramin, apocynin, diphenyleneiodonium chloride and ebselen.

The macrophage has numerous immune functions. Phagocytosis, cytokine release, antigen presentation and reactive oxygen species production all play important parts of the macrophage's role in host defense. More specifically, research on reactive oxygen species has revealed numerous functions ranging from damage to foreign cells and tissue, to acting as secondary messengers.

1.3 Reactive Oxygen Species (ROS)

1.3.1 Introduction

While oxygen is indispensible for the cell to generate ATP, it is also transformed into highly reactive forms, reactive oxygen species (ROS), which can be toxic (Haddad, 2002). Reactive oxygen species are classically defined as oxygen-containing radicals capable of independent existence with one or more unpaired electrons. The term ROS, however, is often expanded to include reactive oxygen-containing compounds without unpaired electrons (Battin et al., 2009). Major sources of ROS include mitochondrol oxidative metabolism (Haddad, 2002), and byproducts of the enzymes xanthine oxidase, lipoxygenase and cyclooxygenase (Masella et al.,

2005). Examples of important ROS encountered in the human body include superoxide anion ($O_2\bullet^-$), hydrogen peroxide (H_2O_2), hydroxyl radical ($OH\bullet$), and peroxynitrite ($OONO^-$):

1.3.2   Reactive Oxygen Species

1.3.2.1   Superoxide Anion ($O_2\bullet^-$)

The one electron reduction of ground state molecular oxygen produces superoxide ($O_2\bullet^-$) (Benzie, 2000):

$$e^- + O_2 \rightarrow O_2\bullet^-$$
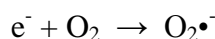
Superoxide radicals are generated within the mitochondrial electron transport chain or, to a lesser extent, via certain enzymes of phagocytic cells like xanthine oxidase and NADPH oxidase (Karihtala et al., 2007). It is thought that 1-5% of total oxygen consumption in aerobic metabolism produces the superoxide radical (Karihtala et al., 2007), which is considered a highly reactive molecule (Hanukoglu, 2006).

1.3.2.2   Hydrogen Peroxide (H_2O_2)

Hydrogen peroxide may be formed either spontaneously from molecular oxygen in peroxisomes or, more usually, via the catalytic activity of superoxide dismutase (SOD) (Karihtala et al., 2007), in which SOD catalyzes the electron reduction of two superoxide radicals leading to the production of hydrogen peroxide (H_2O_2):

$$2O_2\bullet^- + 2H^+ \rightarrow H_2O_2 + O_2$$
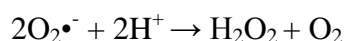
Hydrogen peroxide is not a radical species, is relatively stable and unlike $O_2\bullet^-$, can readily diffuse across cell membranes (Benzie, 2000). An important property of hydrogen peroxide is its ability to generate other ROS, such as the hydroxyl radical (see below).

1.3.2.3   Hydroxyl Radical ($OH\bullet$)

The combination of the ROS hydrogen peroxide and superoxide lead to the formation of the hydroxyl radical, via the Haber-Weiss reaction:

$$H_2O_2 + O_2\bullet^- \rightarrow OH\bullet + OH^- + O_2$$
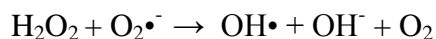
This reaction is very slow in aqueous solutions unless free transition metal ions, such as Fe^{2+} or Cu^{+}, are present, in which case the reaction (known as the Fenton reaction) proceeds very quickly (Benzie, 2000):

$$\text{Metal} (_{ox}) + O_2\bullet^- \rightarrow \text{Metal} (_{red}) + O_2$$

$$\text{Metal} (_{red}) + H_2O_2 \rightarrow \text{Metal} (_{ox}) + OH\bullet + OH^-$$
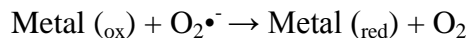
giving an overall reaction of (in the presence of a metal catalyst):

$$H_2O_2 + O_2\bullet^- \rightarrow OH\bullet + OH^- + O_2$$
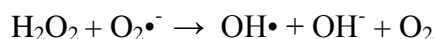
Only picograms of ferrous iron are needed to catalyze the Fenton reaction (Karihtala et al., 2007), however, hydroxyl radical generation is 50 times faster with copper than iron (Battin et al., 2009). Due to its unstable electron structure (Karihtala et al., 2007), attempts to trap OH• can be confounded by the propensity of this radical to react virtually instantaneously with whatever is present at its site of formation (Halliwell, 1999).

1.3.2.4 Peroxynitrite (ONOO⁻)

In inflamed tissues, cells will generate superoxide ($O_2\bullet^-$) and nitric oxide (NO•) radicals that react to form peroxynitrite (Battin et al., 2009):

$$2O_2\bullet^- + NO\bullet \rightarrow ONOO^-$$
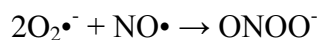
The reactivity of ONOO⁻ is comparable to that of OH• (Karihtala et al., 2007).

1.3.3 Damage to Tissues

The consequences of a mismatch between the production of the reactive oxygen and nitrogen species, and the ability to neutralize their oxidative effect is oxidative damage (Haddad, 2002). Oxidation of lipid, DNA and protein changes the structure and function of these key cellular constituents, and can result in mutation, cell damage or death (Benzie, 2000). Thus, ROS damage has been postulated as the underlying cause of cancer, inflammatory diseases and neurodegenerative diseases (Battin et al., 2009), and is the primary cause of cell death and tissue damage resulting from heart attack and stroke (Perron et al., 2009).

1.3.3.1 H_2O_2

Interest in H_2O_2 is focused on its ability to generate ROS, in particular the hydroxyl radical (OH•). Studies investigating the negative effects of hydrogen peroxide have found that prolonged treatment with H_2O_2 significantly enhanced matrix metalloproteinase (MMP) production *in vitro*. H_2O_2 has been found in large amounts in several human carcinoma cell lines (Karihtala et al., 2007).

1.3.3.2 OH•

The hydroxyl radical is highly reactive and is associated with inducing extensive intracellular damage (Benzie, 2000). OH• oxidize lipids, proteins, and nucleic acids (Battin et al., 2009). Numerous studies have demonstrated the direct effect of the OH• on DNA bases, particularly guanine and adenine, where it produces hydroxylated and ring-opened structures. Pyrimidines have also been found to be susceptible (Halliwell, 1999). Due to the dependence of OH• formation on metal ions, disruptions of metal homeostasis and increases in non-protein-bound metal ion concentrations cause significant increases in OH• generation and oxidative stress (Battin et al., 2009). Iron-mediated oxidative DNA damage by OH• is the primary cause of cell death, under oxidative stress conditions, for both prokaryotes and eukaryotes (Perron et al., 2009).

1.3.3.3 $O_2•^-$

Owing to its charged nature, $O_2•^-$ cannot leave cells by simple diffusion (Benzie, 2000). Studies investigating the role of $O_2•^-$ in disease development have implicated $O_2•^-$ in cancer, inflammatory, cardiovascular and neurodegenerative diseases. Superoxide alone, however, is not capable of directly damaging DNA (Battin et al., 2009).

1.3.3.4 $OONO^-$

Peroxynitrite is known to cause DNA damage and lipid oxidation, and has been implicated in aging associated tissue damage (due to damage of guanine repeats in telomeres), joint disease (caused by decreased production of collagen) and cardiovascular disease (due to decreased availability of nitric oxide) (Battin et al., 2009). Peroxynitrite has been associated with

triggering lipid peroxidation, inducing transversion mutations and DNA strand breaks, disturbing the mitochondrial respiratory chain, and effecting phosphorylation of proteins (Karihtala et al., 2007).

1.3.4   Antioxidant Mechanisms

In general terms, an antioxidant is anything which can prevent or inhibit oxidation. This can be achieved by preventing the generation of ROS, or by inactivating ROS (Benzie, 2000). Antioxidant and other cell redox state modulating enzyme systems act as first-line defense against ROS both intra- and extracellularly (Karihtala et al., 2007). The key antioxidant defenses in the human body are thought to include superoxide dismutase (SOD) and glutathione peroxidase (Halliwell, 1999), followed by other defenses such as transferrin, ferritin, caeruloplasmin, nitric oxide, catalase, peroxiredoxins and scavengers.

1.3.4.1   Superoxide Dismutase (SOD)

The toxicity of the superoxide radical is greatly diminished by the antioxidant metalloenzyme SOD, which catalyzes the reduction of $O_2 \bullet^-$ to less reactive H_2O_2 and O_2. Three different isoforms of SOD have been identified in humans, all of which contain metal ions (copper, zinc or manganese) (Battin et al., 2009), with MnSOD primarily found in mitochondria, CuZnSOD in cytosol (Halliwell, 1999), and ECSOD extracellularly (Karihtala et al., 2007). Mutations in SOD have been implicated in amyotrophic lateral sclerosis, increased susceptibility to Type 2 diabetes, cancer and Alzheimer's disease (Battin et al., 2009). Most $MnSOD^-$ mice die soon after birth with lung damage, while those that survive suffer severe neurodegeneration. Mice that are lacking CuZnSOD seem to be able to survive, but have been found to have difficulty reproducing (Halliwell, 1999).

1.3.4.2   γ-glutamylcysteinylglycine (GSH) and Glutathione Peroxidase (GPx)

γ-glutamylcysteinylglycine (GSH) is the major nonenzymatic regulator of intracellular redox homeostasis, present in all cell types at millimolar concentration. The protein exists either in reduced (GSH) or oxidized (GSSG) form. Under normal cellular redox conditions, the major portion of this regulator is in its reduced form and is distributed in the nucleus, endoplasmic

reticulum and mitochondria. In addition, GSH may be covalently bound to proteins, functioning as a coenzyme during cell defense. Therefore, GSH can either directly scavenge free radicals and/or act as a substrate for proteins like Glutathione Peroxidase (GPx) (Masella et al., 2005). In animals glutathione peroxidase (GPx) acts in co-operation with endogenous tripeptide glutathione (GSH), which is a specific co-factor for hydrogen donation, in the following reaction (Benzie, 2000):

glutathione peroxidase (GPx): $2GSH + H_2O_2 \rightarrow GSSG + 2H_2O$

The oxidized form of glutathione (GSSG) is reduced, and so recycled, by glutathione reductase (GRD) enzymes, and NADPH as a reductant:

glutathione reductase (GRD): $GSSG + NADPH + H^+ \rightarrow 2GSH + NADP^+$

During aging, cellular concentrations of GSH decrease, a characteristic associated with increasing oxidative damage (Battin et al., 2009). In addition, GPx$^-$ mice are more sensitive to toxins, such as paraquat, that generate free radicals and increase heart sensitivity to hypoxia-reperfusion injury (Halliwell, 1999).

1.3.4.3   Transferrin, Ferritin and Caeruloplasmin

Iron and copper are powerful promoters of free radical reactions (Halliwell, 1999). Therefore, finding ways to bind and inactivate these metals could reduce hydroxyl radical production. Proteins found to bind and inactivate these metals include blood transferrin for iron, metallothionein for zinc and cadmium, and metallochaperones like ceruloplasmin for copper (Battin et al., 2009). Mice with spontaneous mutation affecting splicing of the transferrin gene were found to die, unless periodically injected with transferrin (Halliwell, 1999).

1.3.4.4   Catalase

Catalase enzymes, which are found in almost all aerobic organisms, are restricted largely to peroxisomes, and catalyze removal of H_2O_2 via the following reaction (Benzie, 2000):

$2H_2O_2 \rightarrow 2H_2O + O_2$
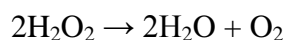
Acatalasemic mice with simultaneous restriction of nutritional vitamin E have been reported to have an elevated incidence of mammary tumors. In humans, decreased catalase activity has been found both in blood samples and in tumor tissue of breast cancer patients. However, the role of decreased catalase in breast tumor formation is controversial as increased catalase levels have also been reported from breast cancer tissues (Karihtala et al., 2007).

1.3.4.5 Peroxiredoxins

As in catalase and glutathione peroxidases, the main function of peroxiredoxins (Prx) is to reduce alkyl hydroperoxides and H_2O_2 to the corresponding alcohol and water. Prxs contain one (Prx VI) or two (Prxs I-V) cysteines as their active site. Compared with catalase, which is present almost entirely in peroxisomes, Prxs are widely distributed in cytosol, peroxisomes, lysosomes, endoplasmic reticulum, Golgi apparatus, and mitochondria. Prx VI knock-out mice suffer from severe lung injury, demonstrating increased sensitivity to hyperoxia, while Prx I over expression has been reported in various human primary tumors (Karihtala et al., 2007).

1.3.4.6 Scavengers

Scavengers are small molecules which interact with primary ROS, such as $O_2^{\bullet-}$ or with secondary reactive species such as carbon-centered lipid radicals. Examples include ascorbic acid (vitamin C) and the lipid soluble and membrane bound tocopherols and tocotrienols (vitamin E) (Benzie, 2000). A simplified overview of some of the above reactions is demonstrated below (figure 3):

Figure 3: Summary of Synthesis and Breakdown of Hydrogen Peroxide

$$H_2O + O_2$$

Mitochondral Electron Transport Chain

Xanthine Oxidase

NADPH Oxidase

$O_2 \bullet^-$

MnSOD
CuZnSOD
ECSOD

Catalase
Prx

H_2O_2

Cu^+/Fe^{2+}

$OH \bullet + OH^-$

GPx

GSSG

GSH

GRD

NADPH + H$^+$

NADP$^+$

$$H_2O$$
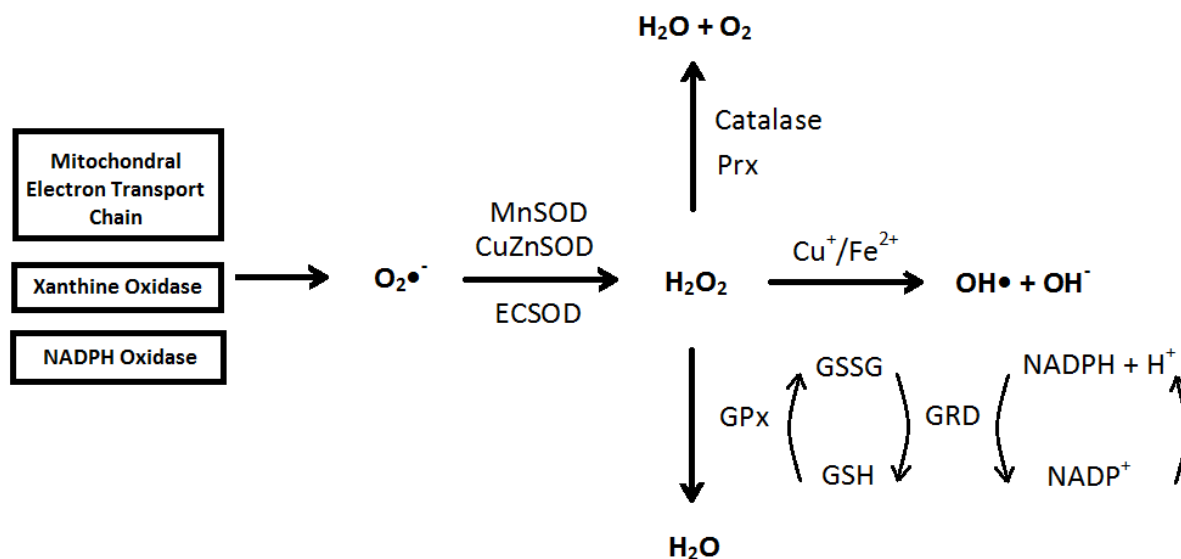
The cell is capable of producing many different reactive oxygen species. These species have been documented to cause serious damage to their surrounding environment, and it is thanks to a cell's inherent antioxidant mechanisms that it can continue to function normally. One prime example of a reactive oxygen species that is capable of leading to cellular damage is hydrogen peroxide, however, this ROS has also been found to play additional vital roles *in vivo* (Masella et al., 2005).

1.4 Hydrogen Peroxide

1.4.1 Introduction

It is well established that high ($\geq$50 µM) levels of H_2O_2 as being cytotoxic to a wide range of animal, plant and bacterial cells (Roy et al., 2006; and Halliwell et al., 2000). It is therefore widely thought that H_2O_2 is very toxic *in vivo* and it seems logical that it should be rapidly eliminated, for example by employing enzymes such as catalases, peroxidases and thioredoxin-linked systems (Halliwell et al., 2000). However, recent research has shed light on possible beneficial effects of hydrogen peroxide on healing and intracellular signaling.

1.4.2 Effects on Healing

Different concentrations of H_2O_2 have been found to have profoundly different biological effects. Roy et al (2006) created full-thickness excisional wounds in mice, which were then treated with either low dose H_2O_2 (1.25 μmol/wound qd for 4 days), high dose H_2O_2 (25 μmol/wound qd for 4 days) or saline (control). It was demonstrated that there was significantly better wound closure over 3 days when using low dose H_2O_2 over saline, and significantly worse wound closure when using high dose H_2O_2 (0-6 days) over low dose H_2O_2, or control (0-10 days). Significantly higher Flt-1 and VEGF mRNA expression were observed at wound edge as well as improved blood flow in lose dose H_2O_2 treated wounds. Monocyte Chemotactic Protein-1 (MCP-1) deficient mice treated with saline were found to have impaired wound angiogenesis and healing, whereas low dose H_2O_2 treated mice demonstrated significantly better wound healing. In addition, mice deficient in p47[phox], an essential subunit of NADPH oxidase, demonstrated abnormal wound closure, which was completely corrected using lose dose H_2O_2.

1.4.3 Intracellular Signaling

Levels of H_2O_2 in the range 20-50 μM or less have demonstrated limited cytotoxicity to many cell types. Indeed, there is growing literature indicating that H_2O_2 can be used as an inter- and intra-cellular signaling molecule (Halliwell et al., 2000). The specificity of hydrogen peroxide as a second messenger comes from its reactions with specific, "oxidation prone" protein Cys residues (Forman et al., 2010A). These targets must be close in proximity to hydrogen peroxide, due to the abundant presence and high catalytic rates of peroxiredoxins (Prx) and glutathione peroxidase (GPx) (Forman et al., 2010B). Signaling pathways activated by hydrogen peroxide include those that stimulate cell proliferation, differentiation, migration or apoptosis (Veal et al., 2007).

In an early experiment by Schreck et al (1991), Jurkat T cells were incubated in the presence of H_2O_2. Results demonstrated that 30-150μM H_2O_2 was found to activate the transcription factor NF-κB, with maximal stimulation between 50-150μM H_2O_2. In addition, H_2O_2 was specific for NF-κB, but not for other transcription factors such as AP-1/c-fos or glucocorticoid receptors.

NAC was found to block the induction of NF-κB, when agents known to induce NF-κB (PMA, TNFα, H_2O_2, poly(rI)-poly(rC) and cycloheximide) were used.

In a subsequent study by Meyer et al (1993), HeLa cells treated with 150μM H_2O_2 led to a 15-fold increase in κB-dependent transactivation of the CAT reporter gene, while treatment with 120nM PMA (an activator of NF-κB and AP-1) gave an almost 60-fold induction. A combination of H_2O_2 and PMA gave a 130-fold induction, which was significantly higher than the induction observed with either stimulus alone. The synergistic effect of the two stimuli was also reflected at the level of DNA binding. Both pyrollidine dithiocarbamate (PDTC) and NAC were found to interfere with the activation of NF-κB by PMA in HeLa cells.

Experiments conducted on the effects of hydrogen peroxide on p53-regulated gene expression indicate that the transcription factor activates antioxidant genes at low, sublethal concentrations of H_2O_2 (0.2mM), whereas, pro-oxidant target genes are activated at increased hydrogen peroxide levels (1.0mM) (Veal et al., 2007; and Sablina et al., 2005).

Research on *S. Pombe* yeast has demonstrated that at low levels of hydrogen peroxide (0.2mM), the peroxiredoxin ,Tpx1, and hydrogen peroxide work together to oxidate and activate the transcription factor Pap1. However, when hydrogen peroxide levels are high (1.0mM), Tpx1 is inhibited, preventing activation of Pap1, yet allowing increased activation of the transcription factor, Atf1, in the nucleus (Veal et al., 2007; and Bozonet et al., 2005).

Studies by Forman et al (2010A; and 2010B) have concluded that hydrogen peroxide also acts as a signaling molecule for: the activation of nuclear factor OxyR (via the formation of cysteinsulfenic acid); the activation of ASK1 (an upstream protein kinase kinase kinase in the $p38^{MAPK}$ and Jun N-terminal kinase (JNK) pathways) via the oxidation of the ASK1 inhibitor, Trx; and the activation of cyclooxygenase and lipoxygenase.

The role of hydrogen peroxide in healing and as an intracellular second messenger has opened new avenues of research for a chemical that was once considered as having a purely destructive role in tissues. These new findings have lead to the need for new and improved methods of detection that are both sensitive and specific enough for hydrogen peroxide.

1.5   ROS Detection Methods

1.5.1   Introduction

The number and specificity of tests for ROS detection has increased over time. Detection reagents specific to certain ROS can now be used for experimentation, as opposed to tests which detect multiple ROS at once. Examples of recently developed tests specific to H_2O_2 detection include: Amplex Red; the Fox Method; 3, 5, 3', 5'-tetramethylbenzidine (TMB); monoboronated 2-methyl-4-methoxy Tokyo Green (PG1) and monoboronated resorufin (PC1); and SNAP-tag Protein Labeling.

1.5.2   Amplex Red [N-acetyl-3,7-dihydroxyphenoxazine]

Amplex Red is a colourless, nonfluorescent derivative of dihydroresorufin (Zhou et al., 1997), and belongs to the "positive" fluorogenic probes family, which consist of compounds that are non-fluorescent (or weakly fluorescent), but yield fluorescent products upon reaction with reactive oxygen species (ROS) (Bartosz, 2006). In the presence of Horse Radish Peroxidase (HRP), H_2O_2 is decomposed to the hydroxyl radical, which is then reduced to water as a result of irreversible chemical oxidation of Amplex Red (Rhee et al., 2010). The product is the fluorescent molecule known as Resorufin (figure 4), which exhibits a maximum excitation wavelength 563nm and maximum emission wavelength of 587nm (Zhou et al., 1997).

Figure 4: Oxidation Reaction of Amplex Red
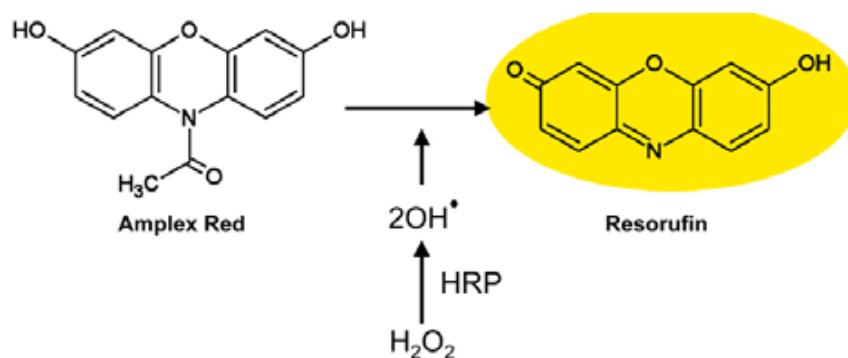
Studies using Amplex Red as a detection reagent have demonstrated it to be highly stable, with a reaction stoichiometry of 1:1 (Zhou et al., 1997), as long as the ratio of Amplex Red: H_2O_2 in the

reaction mixture is higher than 5 (Mohanty et al., 1997). On account of its minimal background fluorescence, Amplex Red can detect levels of H_2O_2 as low as 2-5 pmol (Mohanty et al., 1997), and is 5-20 times more sensitive in detecting H_2O_2 than scopoletin (Zhou et al., 1997). In addition, Amplex Red has been found to be selective for H_2O_2 over superoxide (Zhou et al., 1997), and specific to extracellular detection (Mohanty et al., 1997). Disadvantages include the conversion of resorufin to the non-fluorescent product resazurin (Mohanty et al., 1997) when the ratio of H_2O_2 to substrate is greater than 1 (Zhou et al., 1997) (figure 5),

Figure 5: Oxidation of Amplex Red to Fluorescent Resorufin and Non-Fluorescent Resazurin

N-Acetyl-3,7-Dihydroxyphenoxazine
(A6550)
(Non-fluorescent)

7-Hydroxy-3H-Phenoxazine-3-one
(Resorufin)
(Highly Fluorescent)
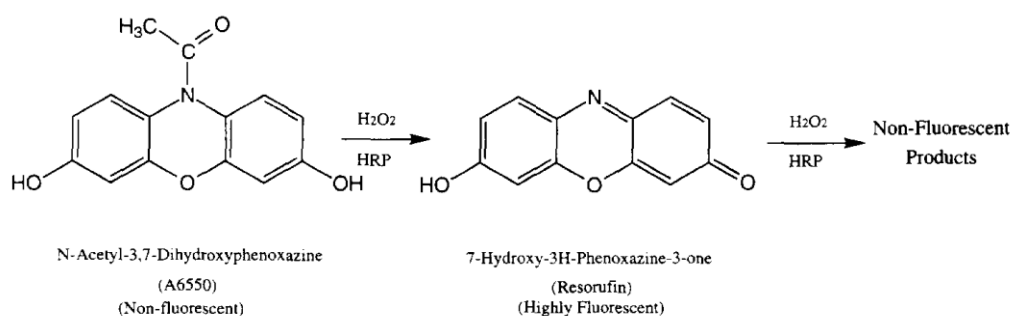
and the possible unwanted oxidation of Amplex Red by other oxidizing agents such as peroxidases and myeloperoxidases (Mohanty et al., 1997).

1.5.3 Fox Method

In dilute acid, H_2O_2 oxidizes ferrous ion (Fe^{2+}) via the Fenton Reaction:

$$Fe^{2+} + H_2O_2 \rightarrow Fe^{3+} + OH^{\bullet} + OH^{-}$$

The resultant ferric ion (Fe^{3+}) is then able to react with xylenol orange (XO) to produce a blue-purple complex known as o-cresolsulfone-phthalein 3',3''-bis(methylimino) diacetate which is read as absorbance against a XO/Fe^{2+} blank:

$$Fe^{3+} + XO \rightarrow \text{blue-purple complex}$$

By adding sorbitol, the amount of Fe^{3+} is increased to about 15mol per mole of H_2O_2 (Rhee et al., 2010), leading to increased yields of the blue-purple complex, a high extinction coefficient and

therefore an increased sensitivity of the measurement of H_2O_2 by the Fe-XO assay (Gay et al., 2000):

$$Fe^{2+} + H_2O_2 \rightarrow Fe^{3+} + OH^\bullet + OH^-$$

$$sorbitol + OH^\bullet \rightarrow sorbitol^\bullet + H_2O$$

$$sorbitol^\bullet + O_2 \rightarrow sorbitolO_2^\bullet \rightarrow sorbitol(keto) + HO_2^\bullet$$

$$Fe^{2+} + HO_2^\bullet \rightarrow Fe^{3+} + H_2O_2$$
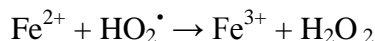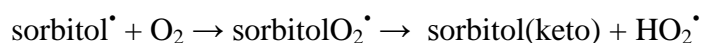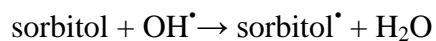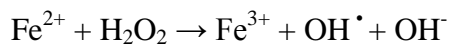
The FOX method is suited for the determination of low levels of H_2O_2 in aqueous media, and allows the detection of 100 pmol of H_2O_2 in a 50 μl sample. In addition, the assay is relatively free from interference by other components often present in test samples (such as protein, trichloroacetic acid and salts). Compounds that bind ferric ions (such as desferrioxamine, diethylenetriamine pentaacetic acid, and ethylenediamine tetraacetic acid) will inevitably interfere with the reaction (through competition with xylenol orange for the generated ferric ions) and should be present at no more than 1 μM in the assay (Rhee et al., 2010).

1.5.4   TMB (3, 5, 3', 5'-tetramethylbenzidine)

The product of the reaction between HRP and H_2O_2, $OH^\bullet$, oxidizes the TMB molecule to produce a cation free radical. This radical is in equilibrium with blue charge-transfer complex with absorption maximum at 653 nm. Further oxidation of the cation free radical via $OH^\bullet$ or mild acidification, leads to the formation of a yellow diimine, with absorbance maximum 450 nm, and a higher extinction coefficient than the blue charge-transfer complex (figure 6). Calculation of H_2O_2 is therefore made by measuring the absorbance of the sample at 450nm, and comparing it to a standard curve.

Figure 6: Chemical Reaction of TMB to Fluorescent Products Diimine Yellow and Charge-Transfer Complex Blue
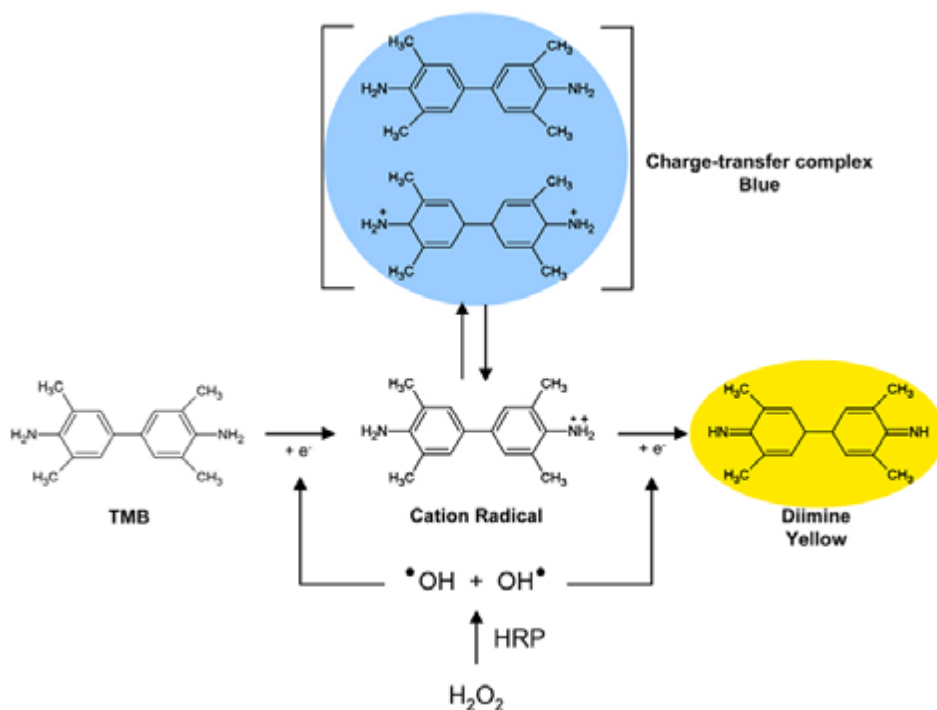
Advantages of this technique include its high sensitivity, good stability at acidic pH, and wide pH range over which HRP is active. Since TMB is photosensitive, it should be stored in the absence of light (Rhee et al., 2010).

1.5.5 PG1 (monoboronated 2-methyl-4-methoxy Tokyo Green) and PC1 (monoboronated resorufin)

In order to avoid oxidative reactions of probes by reactive oxygen species (ROS) other than H_2O_2, different probes have been developed whose functions are not dependent on oxidation (Maeda et al., 2005). Two such probes are PG1 (monoboronated 2-methyl-4-methoxy Tokyo Green) and PC1 (monoboronated resorufin). Both reagents work on the premise of deprotection of aryl boronates by H_2O_2 to phenols (Miller et al., 2007). This deprotection leads to the synthesis of 2-Methyl-4-O-methyl Tokyo Green from PG1 (a 10 fold increase in green fluorescence) and the synthesis of resorufin from PC1 (a 40 fold increase in red fluorescence) (Miller et al., 2007) (figure 7).

Figure 7: Deprotection of PG1 and PC1 to Fluorescent Products
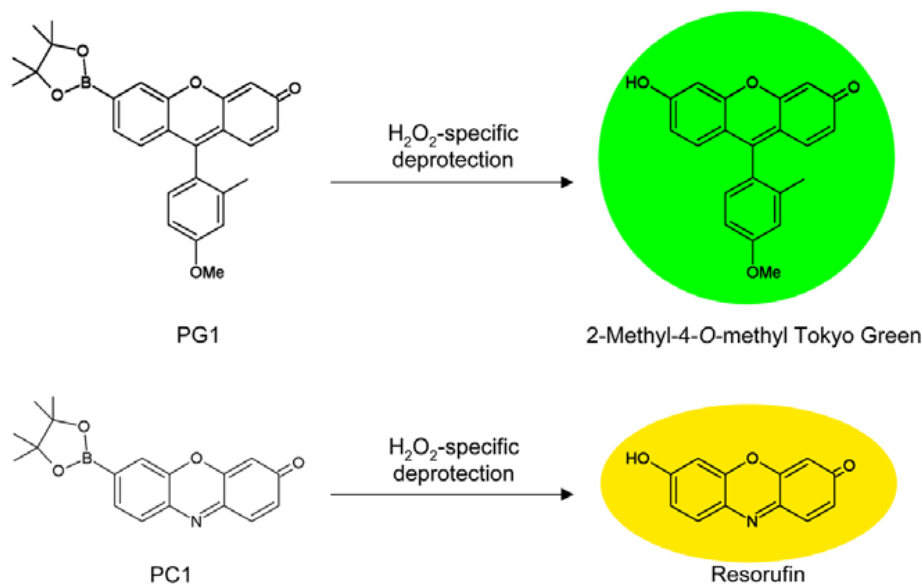
Both PG1 and PC1 show high selectivity for H_2O_2 over other oxidants such as peroxynitrite, hydroxyl radical, lipid peroxidases, nitric oxide, and hypochloride (Rhee et al., 2010). In addition, PG1 and PC1 are capable of entering cells, whereas the deprotected products remain restricted to the intracellular environment (Rhee et al., 2010). These properties can be used to detect natural signaling levels of H_2O_2 generated by living cells and can be used to map molecular pathways associated with H_2O_2 production (Miller et al., 2007). Although PG1 and PC1 are promising tools for the selective monitoring of intracellular H_2O_2 production, they cannot provide spatial and temporal information for H_2O_2 molecules in cellular contexts (Rhee et al., 2010). The reaction of these two probes with H_2O_2 is irreversible, therefore the fluorescence intensities obtained reflect the cumulative total of H_2O_2 molecules produced during a given time interval; the probes cannot be used for the detection of transient changes in H_2O_2 concentration (Rhee et al., 2010).

1.5.6   SNAP-tag Protein Labeling

This technology combines the precision of site-specific labeling, using genetically encodable tags, with the chemical versatility of small-molecule probes (Srikun et al., 2010). SNAP-tags are

quite complex molecules, but can easily be described by breaking them down into 4 components: the probe, the SNAP-tag, AGT, and targeting protein. The probe consists of H_2O_2 detectors such as Peroxy Green 1 or 2 (PG1 of PG2). These probes are covalently bonded to a SNAP-tag substrate like benzylguanine or benzyl-2-chloro-6-aminopyrimidine, thus forming complexes such as SPG1 and SPG2, respectively. The complexes are capable of covalently bonding to another complex consisting of the targeting protein and AGT (O^6-alkylguanine-DNA alkyltransferase) (figure 8). Initially, the targeting protein-AGT complex is incubated with the cells of interest, which targets specific organelles such as the plasma membrane, nucleus, mitochondria, or endoplasmic reticulum (Srikun et al., 2010). SPG1 or 2 is then added, which searches out the targeting protein-AGT complex, and forms a covalent bond between the SNAP-tag and Cys145 of the AGT.

Figure 8: Formation of SNAP-tag Protein, and its Conversion to Fluorescent Product
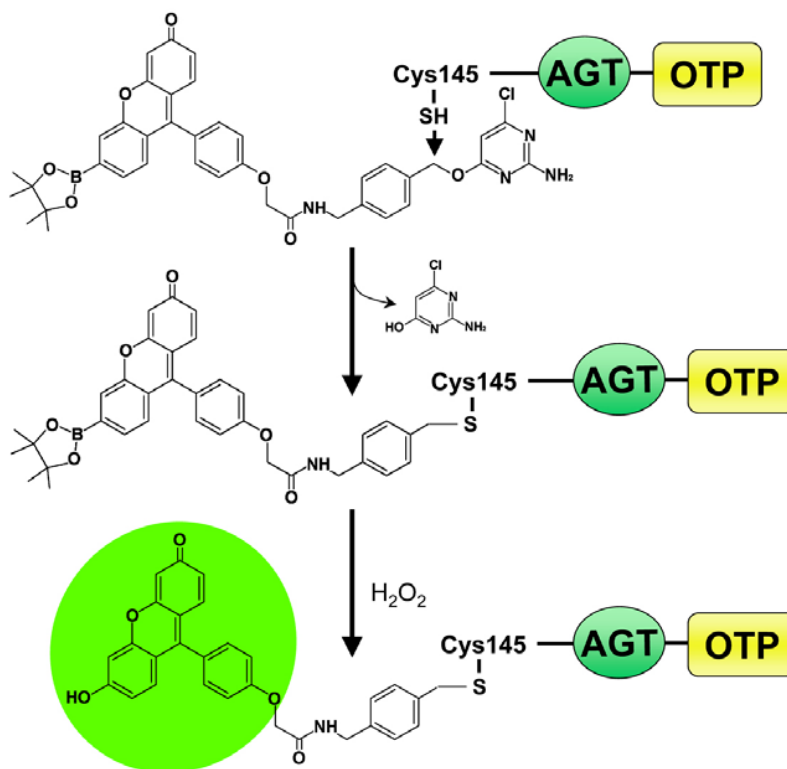
As described above, deprotection of the SPG1 fluorophore by H_2O_2 results in a marked increase in green fluorescence at the target organelle (Rhee et al., 2010), which is read by scanning

confocal microscopy. Experiments by Srikun et al (2010) have demonstrated that the SPG1 probe acts extracellularly, while the SPG2 probe targets intracellular sites, with both probes demonstrating visible absorption bands centered at 465nm and weak fluorescence with an emission maximum of 515nm. Other probes made from detection reagents like Tokyo Green have demonstrated superior quantum yields. An overview of these characteristics are summarized below (table 1):

Table 1: Comparison of Different H_2O_2 Detection Methods

	Amplex Red	Fox Method	TMB	PG1/PC1	SNAP-tag
Site of Detection	Extracellular	Extracellular	Extracellular	Intracellular	Intracellular/ Extracellular
Chemical Reaction	Oxidation	Oxidation	Oxidation	Deprotection	Deprotection
Measurement	Fluorescence	Absorbance	Absorbance	Fluorescence	Fluorescence
Sensitivity	2-5 pmol	100 pmol	10µM	100µM	100µM
Advantages	Good sensitivity; highly stable; active over wide pH range; minimal background fluorescence	Good sensitivity; relatively free from interference; can be performed in acidic conditions	Good stability; active over wide pH range	Not dependent on oxidation; can be used to map molecular pathways	Site-specific labelling; not dependent on oxidation; unbound probe can be washed off
Disadvantages	Can form the non-fluorescent product Resazurin; photosensitive	Compounds that bind ferric irons can interfere with reaction	Photosensitive	Cannot provide spatial or temporal information	Deprotection reaction is irreversible; some products not yet commercially available

1.6   Conclusion

1.6.1   Objective

The objective of this thesis is to gain further understanding of the amount and mechanism of extracellular hydrogen peroxide production of the RAW 264.7 macrophage.

1.6.2   Rationale

Macrophages are one of the first cell lines to come in contact with an implant surface when placed into the oral cavity. The response elicited by these macrophages will dictate whether the implant successfully integrates within the surrounding bone. This response may include the release of reactive oxygen species, such as hydrogen peroxide, which have been associated with foreign cell and tissue destruction, wound healing and cellular messaging.

1.6.3   Hypothesis

The amount of extracellular hydrogen peroxide production in cell culture media will be measured using the Amplex Red detection reagent. It is hypothesized that RAW 264.7 macrophages will produce significantly more hydrogen peroxide than cell free control. In addition, RAW 264.7 macrophages stimulated with LPS will produce significantly more hydrogen peroxide than cells without stimulation.

2 Materials and Methods

2.1 Cell Culture

2.1.1 **RAW 264.7 Cell Line**

The RAW 264.7 cell line has been used extensively in our lab, and is the most commonly used mouse macrophage cell line in medical research (Hartley et al., 2008). RAW 264.7 macrophages have been documented to have properties of normal macrophages including the ability to pinocytose neutral red, phagocytose zymosan and latex beads, kill antibody-coated SRBC targets and secrete lysozyme (Raschke et al., 1978). The decision to utilize RAW 264.7 cells was based on past research demonstrating its ability to produce reactive oxygen species (Kimura K et al., 2008; Yoo HG et al., 2002; and Park et al., 1999).

2.1.2 **Culture Technique**

RAW 264.7 macrophage cells were obtained from American Type Culture Collection, plated on 75 cm^2 culture flasks (BD Falcon, USA) in 10ml of complete media, and incubated at 37°C.

Complete media for cell culture consisted of: 15% Fetal Bovine Serum (Hyclone), which was heat deactivated for 30 minutes at 56-58˚C; 10% antimicrobial supplement which consisted of 440ml Dulbecco's Modified Eagle's Medium, 20ml Fungizone, 0.5g penicillin and 5ml gentamycin sulphate (the contents of which were filtered through 0.045μm and then 0.2μm filters); and 75% Dulbecco's Modified Eagle's Medium (Stemcell Technologies, Canada).

Upon reaching 80% confluency, about 25-30% of macrophages were transferred to a new 75 cm^2 flask, to which a final volume of 10ml complete media was added. This process was repeated until cells were needed for experimentation.

2.1.3 **Determination of Cell Number**

Cell number was determined by adding 1ml of RAW 264.7 cells in complete media to 19ml of isotonic solution in a 35ml vial (Accuvette, Fl, USA), which produced a 0.5ml sample. The vial was then placed into a cell counter (Coulter Counter Z1, England). The count generated was

then multiplied by 40 in order to obtain the number of cells/ml in the original solution. All cell counts were performed in quadruplicate.

2.2   H$_2$O$_2$ Detection

2.2.1   Amplex Red Detection Reagent:

Extracellular H$_2$0$_2$ was detected using an Amplex Red Monoamine Oxidase Assay Kit (A12214, Molecular Probes) with reagent concentrations being adjusted to match that of the Amplex Red Hydrogen Peroxide/Peroxidase Assay Kit (A22188, Molecular Probes). The final Amplex Red working solution consisted of 4.85ml 1x Reaction Buffer, 100µl Horse Radish Peroxidase (HRP, 10U/ml) and 50µl Amplex Red (10mM).

2.2.2   Fluorometry

All H$_2$0$_2$ readings were conducted by adding 50µl of solution containing H$_2$0$_2$ to 50µl of Amplex Red reagent into the well of a black 96 well costar microplate. Plates were then allowed to stand for 30 minutes at room temperature, in the absence of light. The fluorescence was measured on a fluorometer (FLUOstar Optima, BMG Labtech) set at 550nm excitation and 590nm emission.

2.3   Statistical Analysis

Statistical tests included the t-test, one and two factor ANOVA using SPSS version 19 (IBM). Significance for all tests was set at p≤0.05.

3   Results

3.1   Determination of Optimal Conditions for Experimentation

3.1.1   Amplex Red Standard Curve

An Amplex Red standard curve was created in order to determine the relationship between H_2O_2 concentration and fluorescence. H_2O_2 in PBS was varied from 0.08μM to 10μM, and a linear relationship was found between H_2O_2 concentration and fluorescence, with a correlation coefficient of 0.99 (figure 9).

Figure 9: Amplex Red Fluorescent Detection of Different Concentrations of H_2O_2 in PBS
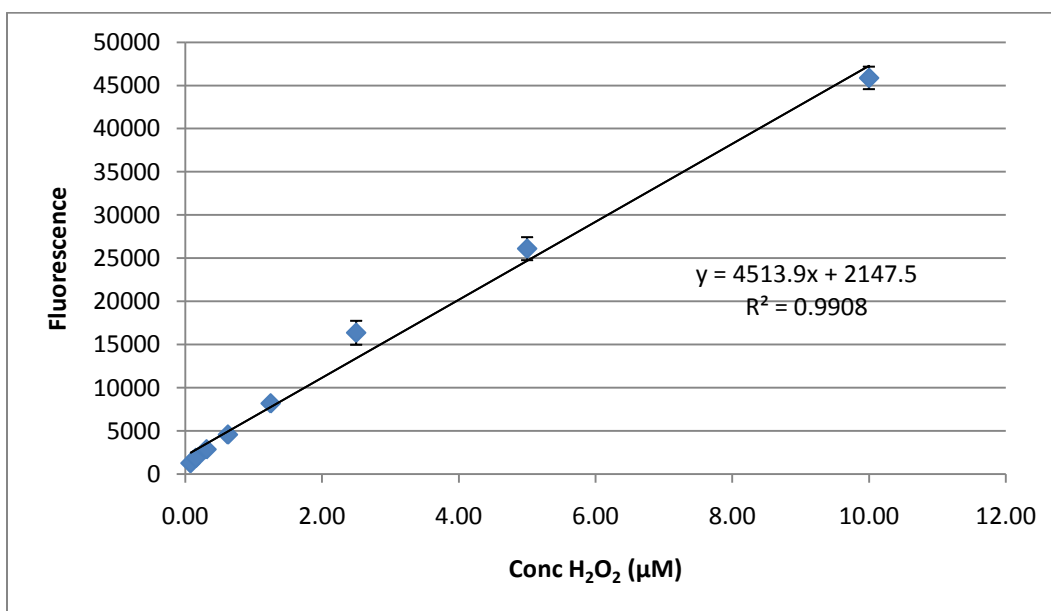
$$y = 4513.9x + 2147.5$$
$$R^2 = 0.9908$$

Concentrations of H_2O_2 ranging from 0.08μM to 10μM were tested using the Amplex Red protocol. All measurements performed at 21°C in the absence of light.

3.1.2   Determination of Optimal Media and Microplate

An experiment was then designed to ascertain which type of media and 96 well microplate were best for measuring Amplex Red fluorescence. Standard curves were performed using PBS, DMEM and complete media in both clear and black 96 well Costar microplates. Statistical analysis demonstrated that in the clear 96 well microplate, concentration of H_2O_2, the type of

medium and the interaction between concentration and medium had statistically significant effects on fluorescence. The various culture solutions produced results that were significantly different, with PBS producing the highest amount of fluorescence, followed by DMEM and then complete media. Similar results were obtained when using the black 96 well plate (figures 10 and 11). When comparing PBS standard curves in black versus clear plates, significantly more fluorescence was detected from the clear plate. Since black microplates limit well-to-well crosstalk (Hidex Personal Life Science; Knight S; and Promega 2011), it was determined that well-to-well crosstalk was occurring between wells in the clear plates, which lead to greater fluorescence output and detection. It was therefore determined that the optimal set-up for measuring H_2O_2 would be using PBS and black 96 Costar microplates.

Figure 10: Comparison of H_2O_2 Standard Curves in Different Solutions within a Clear 96 Well Costar Microplate
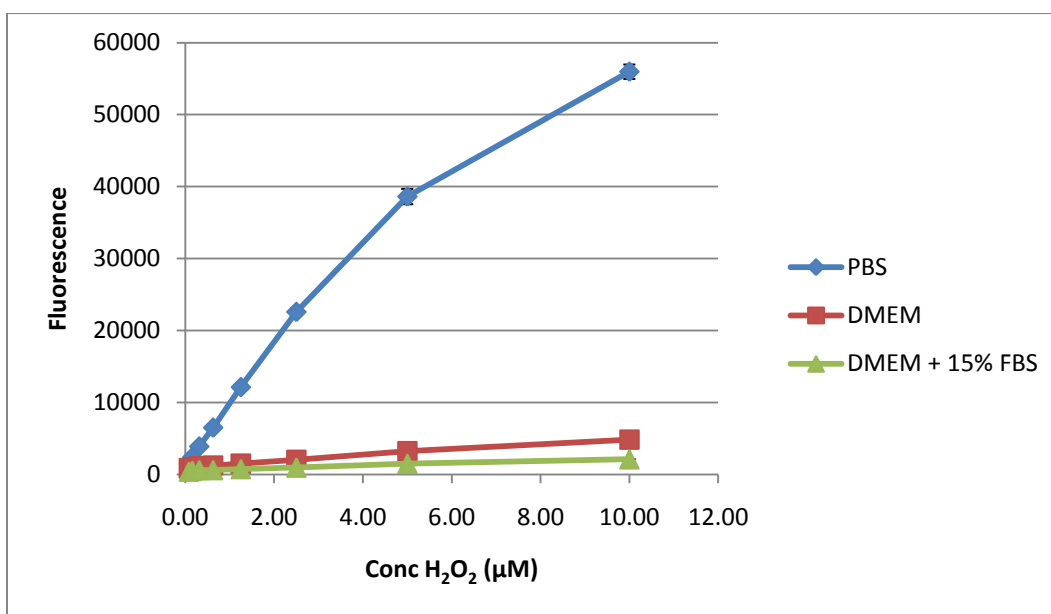
Concentrations of H_2O_2 ranging from 0.08μM to 10μM were tested using the Amplex Red protocol in either PBS, DMEM or DMEM+15% FBS. All measurements were performed in a clear microplate at 21°C, in the absence of light. Fluorescent detection in PBS was statistically significantly higher than DMEM and DMEM+15% FBS, and DMEM was statistically significantly higher than DMEM+15% FBS (p≤0.006).

Figure 11: Comparison of H$_2$O$_2$ Standard Curves in Different Solutions within a Black 96 Well Costar Microplate
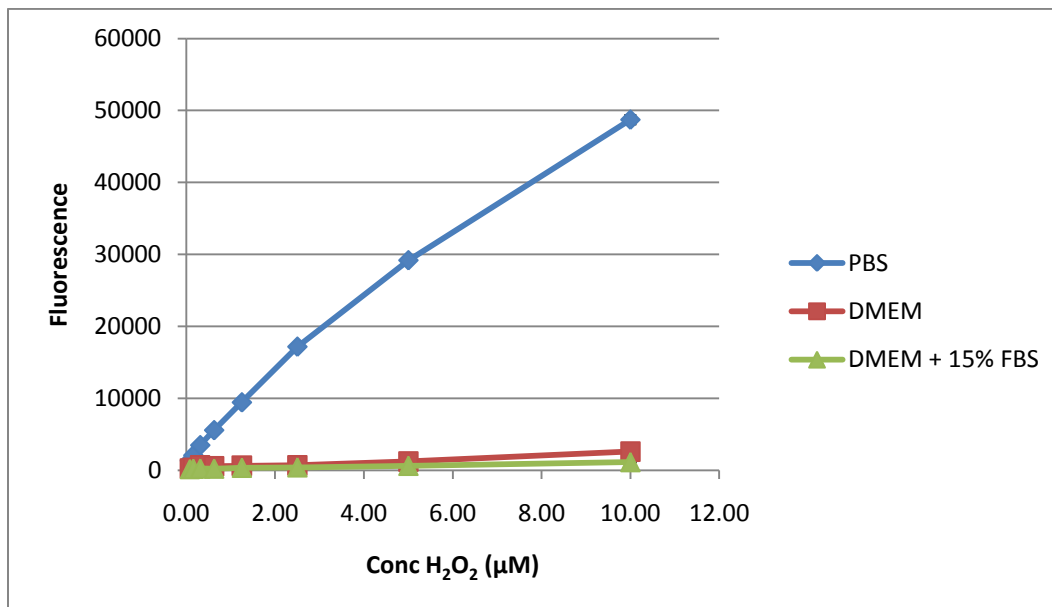
Concentrations of H$_2$O$_2$ ranging from 0.08μM to 10μM were tested using the Amplex Red protocol in either PBS, DMEM or DMEM+15% FBS. All measurements were performed in a black microplate at 21°C, in the absence of light. Fluorescent detection in PBS was statistically significantly higher than DMEM and DMEM+15% FBS, and DMEM was statistically significantly higher than DMEM+15% FBS (p≤0.006).

3.2   Effect of RAW 264.7 Cells on Amplex Red Detection System

3.2.1   Direct Detection of H$_2$O$_2$ from RAW 264.7 Cells

After determining the optimal conditions for experimentation, the following experiment was conducted in order to determine the effect of RAW 264.7 cells on Amplex Red, since previous research had demonstrated that horse radish peroxidase used in the detection reaction could possibly catalyze the oxidation of NADH and glutathione to produce additional amounts of H$_2$O$_2$ (Votyakova et al., 2004). Using a tissue culture plastic (TCP) plate, 4 wells were plated with 1ml of RAW 264.7 cells at a concentration of 1×10^6 cells/ml in complete media, while another 4 wells received 1ml of complete media (control). The number of wells required was based on a

determination of effect size via the d statistic formula, assuming a difference in means was 1000FU, standard deviation = ±250FU, and 5% α level (Mantena et al., 2008; Woo et al., 2004; and Park et al., 1999). The plate was placed in a 37^0C incubator for 6 hours. After 6 hours the complete media was removed and each well was washed 3 times with PBS. Subsequently, each well received 1000µl of Amplex Red solution and was allowed to sit for a further hour at room temperature (21^0C), in the absence of light. The 21^0C temperature was chosen, because it was in agreement with the protocol specified by the manufacturer of Amplex Red, which states that the reaction is to be performed at room temperature. Each well's entire supernatant was then removed and centrifuged at 13,000 rpm for 30 seconds. Three, 100µl samples were then removed from the surface of each centrifuged supernatant, and individually added into the well of a 96 well black Costar microplate. The microplate was inserted into a fluorometer, using the same settings as that for the Amplex Red protocol. Results demonstrated a small, yet statistically significant greater amount of H_2O_2 detected from Amplex Red situated over RAW 264.7 cells (296±13 FU) than control (116±9 FU). This indicated that over a 1 hour period, RAW 264.7 cells produced a small amount of hydrogen peroxide.

3.2.2 Effect of RAW 264.7 Cells on Ability of Amplex Red to Detect Exogenous H_2O_2 Detection

Using the remaining Amplex Red supernatant from the previous experiment, three, 50µl samples/well were obtained and added to 50µl 2.5µM H_2O_2 in a black 96 well microplate, and measured for H_2O_2 following the Amplex Red protocol (figure 12).

Figure 12: Protocol for Determining Effect of RAW 264.7 Cells on Amplex Red Detection System
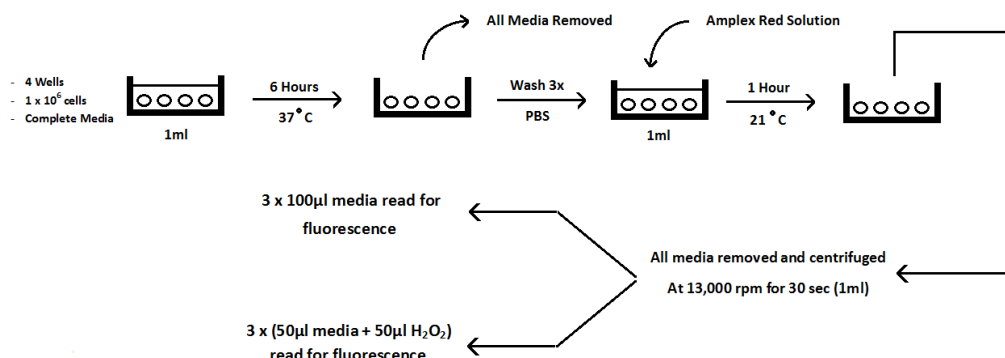
Amplex Red exposed to RAW 264.7 cells for one hour produced significantly less fluorescence in respect to H_2O_2 (11,949±258 FU) than that found in controls (22,013±814 FU), in which the Amplex Red did not contact cells. Thus, it was concluded that for optimal detection, Amplex Red could not be in the same medium as RAW 264.7 cells when measuring hydrogen peroxide, since these cells altered the reagents detection ability.

3.3   Effect of LPS on RAW 264.7 Mediated H_2O_2 Production

3.3.1   Effects of Cells and LPS

Since differences in H_2O_2 production when comparing the presence versus absence of cells was relatively small (previous experiment), an experiment was designed in order to investigate whether the cells could be stimulated by LPS, as LPS is known to increase H_2O_2 levels in macrophages (Kimura et al., 2008; Woo et al., 2004; and Park et al., 1999). RAW 264.7 cells were plated on a 24 well tissue culture plastic plate, in which 8 wells received 1ml cells in complete media at 1×10^6 cells/ml, while another 4 wells contained only 1ml complete media (cell free control). The plate was then incubated for 6 hours at 37^0C. After 6 hours, all wells were washed 3 times with PBS. Control wells then received 500µl PBS, while 4/8 wells with cells received 1µg/ml *E.coli* LPS serotype 055:B5 (Sigma-Aldrich, St. Louis, MO, USA) in

500µl PBS, and the remaining 4 wells with cells received only 500µl PBS. The plate was returned to the incubator where 100µl was taken from each well and placed into a 2ml Eppendorf tube at 1, 3 and 6 hours. Each tube was centrifuged at 13,000 rpm for 30 seconds. A 50µl sample of centrifuged supernatant solution was then removed as close to the surface as possible, and added to 50µl Amplex Red in a black 96 well Costar microplate. H_2O_2 measurements were then performed following the Amplex Red protocol (figure 13).

Figure 13: Protocol for Determining Effect of LPS on RAW 264.7 Mediated H_2O_2 Production
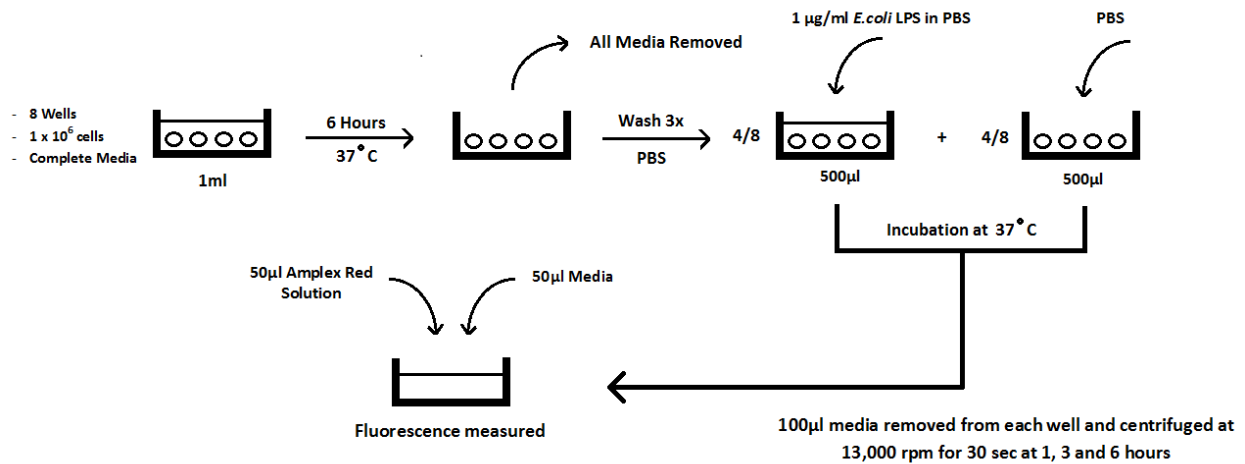
When comparing the amount H_2O_2 depleted in the presence/absence of cells, it was found that time, cells, and the interaction between time and cells all had significant effects. More specifically, there was significantly more depletion of H_2O_2 in wells with cells, compared to those without. In addition, there was no statistical difference in H_2O_2 depletion between RAW 264.7 cells that were/weren't treated with LPS (figure 14).

Figure 14: Influence of RAW 264.7 Macrophages and *E.coli* LPS on H$_2$O$_2$ Detection by Amplex Red
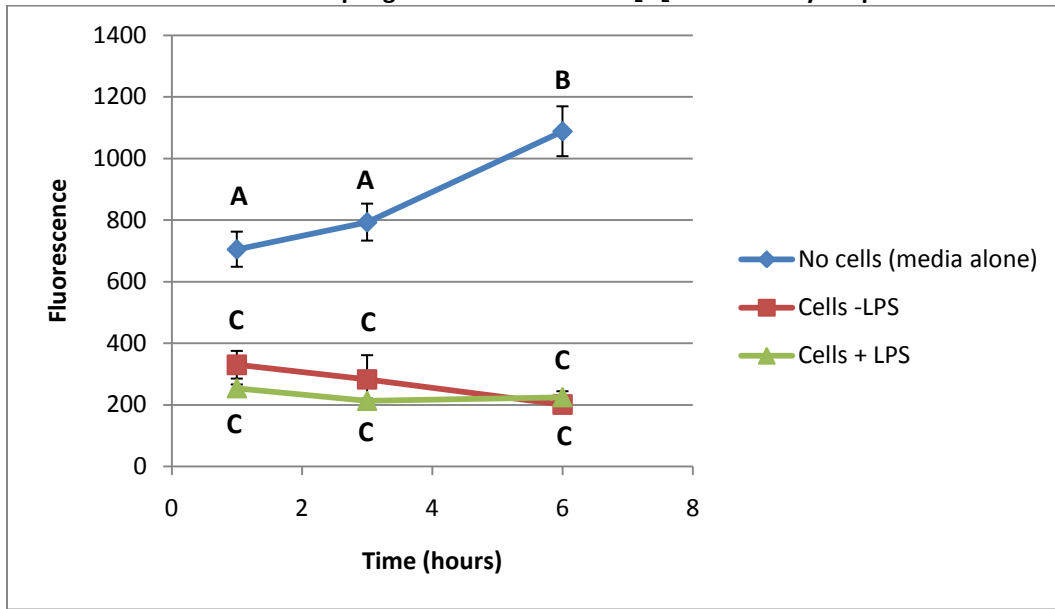
1x10^6 cells/well (+/- LPS) and control were incubated at 37^{0}C and tested for H$_2$O$_2$ using Amplex Red at 1, 3 and 6 hours, in the absence of light. Different alphabetic letters represent statistically significant differences in fluorescent detection (p≤0.008).

3.3.2 Detection of Extra- and Intracellular H$_2$O$_2$ Production

Since the previous experiment demonstrated that LPS had no effect on extracellular hydrogen peroxide production, an experiment was designed to investigate whether LPS stimulation of H$_2$O$_2$ could be demonstrated intracellularly. Using a 24 well TCP plate, 8 wells were plated with 1ml of RAW 264.7 cells at 1x10^6 cells/ml in complete media, while another 4 wells received only 1 ml of complete media (control). The plate was then placed in a 37^{0}C incubator for 6 hours. Following 6 hours of incubation, all wells were washed 3 times with complete media. Subsequently, 4/8 wells with cells received 1µg/ml *E.coli* LPS in 500µl complete media, while all remaining wells, regardless of presence of cells, received 500µl of complete media. The plate was then incubated for 20 hours at 37^{0}C. After 20 hours, all wells were washed 3 times with PBS, refilled with 500µl PBS, and allowed to incubate for 4 hours at 37^{0}C. Following 4 hours of incubation, each well had all of its PBS removed and centrifuged at 13,000 rpm for 30 seconds. 50µl was then removed from the surface of each supernatant and read for H$_2$0$_2$ using the Amplex Red protocol. The 24 well TCP plate, with RAW 264.7 cells still remaining on its surfaces, was

then placed in a freezer which induced cell lyses. After 20 minutes, the plate was removed, and each well containing lysed cells was filled with 500µl of PBS for 2 minutes. The PBS was collected, centrifuged at 13,000 rpm for 30 seconds and sampled for intracellular H_2O_2 using the Amplex Red protocol. Results demonstrated that there was no significant effect of LPS on extra- (-LPS = 204±35 FU; +LPS = 236±43 FU) or intracellular (-LPS = 188±68 FU; +LPS = 237±138 FU) H_2O_2 levels. One way ANOVA and post hoc analysis indicated that the only significant difference in H_2O_2 depletion was that between control and all groups with cells (figure 15).

Figure 15: Comparison of RAW 264.7 Macrophage Extracellular Versus Intracellular H_2O_2 Content
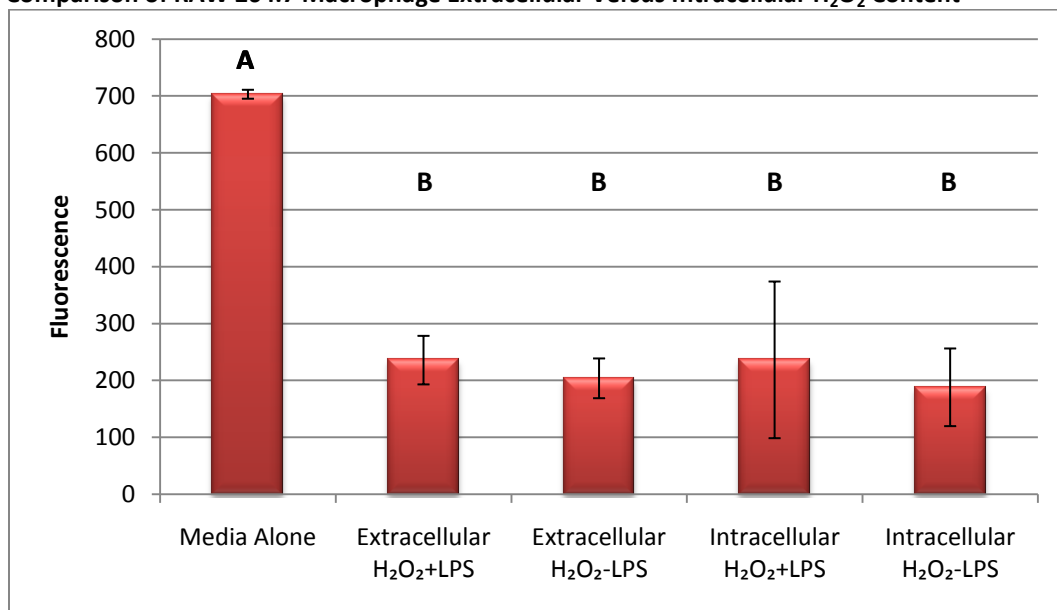
Wells (+/- $1x10^6$ cells/well) were incubated at 37°C for 24 hours +/- LPS and read for extracellular H_2O_2 using the Amplex Red protocol, in the absence of light. Cells were then transferred to a -20°C environment for 20 minutes, which lysed the cells, thus permitting intracellular H_2O_2 detection. Different alphabetic letters represent statistically significant differences in fluorescent detection (p≤0.05).

3.4 Effect of RAW 264.7 Cells on H_2O_2 Depletion

Since previous experiments demonstrated that the presence of RAW 264.7 cells lead to reduced values of fluorescence relative to cell free controls, the following experiment was conducted in order to investigate whether RAW 264.7 cells deplete exogenously added H_2O_2. Using a 24 well TCP plate, 4 wells were plated with 1ml of RAW 264.7 cells at a concentration of $1x10^6$ cells/ml

in complete media, while another 4 wells received 1ml of complete media (control). The plate was placed in a 37^0C incubator for 6 hours. Subsequently, all wells were washed 3 times with PBS, and then filled with 500µl of 2.5µM H_2O_2 in PBS, and allowed to incubate for 4 hours. After 4 hours, the supernatant from each well was removed, placed in an Eppendorf tube, and centrifuged at 13,000 rpm for 30 seconds. Three, 50µl samples/tube were then removed from the surface of each supernatant and read for presence of H_2O_2 using the Amplex Red protocol. Results demonstrated that wells with cells depleted a significant amount of H_2O_2 (257±39 FU) compared to cell free control, which did not demonstrated any depletion (19877±381 FU).

3.5   Effect of RAW 264.7 Cell Concentration on H_2O_2 Depletion

The affects of differences in RAW 264.7 cell number, as well as incubation temperature, were then examined.

3.5.1   Four Hour Incubation Period

Using a 24 well TCP plate, RAW 264.7 cells were plated in triplicate at different concentrations ($1x10^6$, $5x10^5$, $2.5x10^5$, $1.25x10^5$, $6.25x10^4$ cells/ml, as well as a control) in 1ml of complete media. The plate was placed in a 37^0C incubator for 6 hours, after which time the wells were washed 3 times with PBS. Subsequently, each well was filled with 500µl 2.5µM H_2O_2 and incubated for 4 hours at 37^0C. After 4 hours the supernatant was removed, placed in an Eppendorf tube, and centrifuged at 13,000 rpm for 30 seconds. A 50µl sample/tube was then removed near the surface of the supernatant and read for H_2O_2 using the Amplex Red protocol. After 4 hours, there was no difference in H_2O_2 depletion between wells with cells, however, these wells all produced significantly more H_2O_2 depletion than control (figure 16).

Figure 16: Effect of Raw 264.7 Macrophage Cell Number on Extracellular H$_2$O$_2$ Depletion after Four Hours
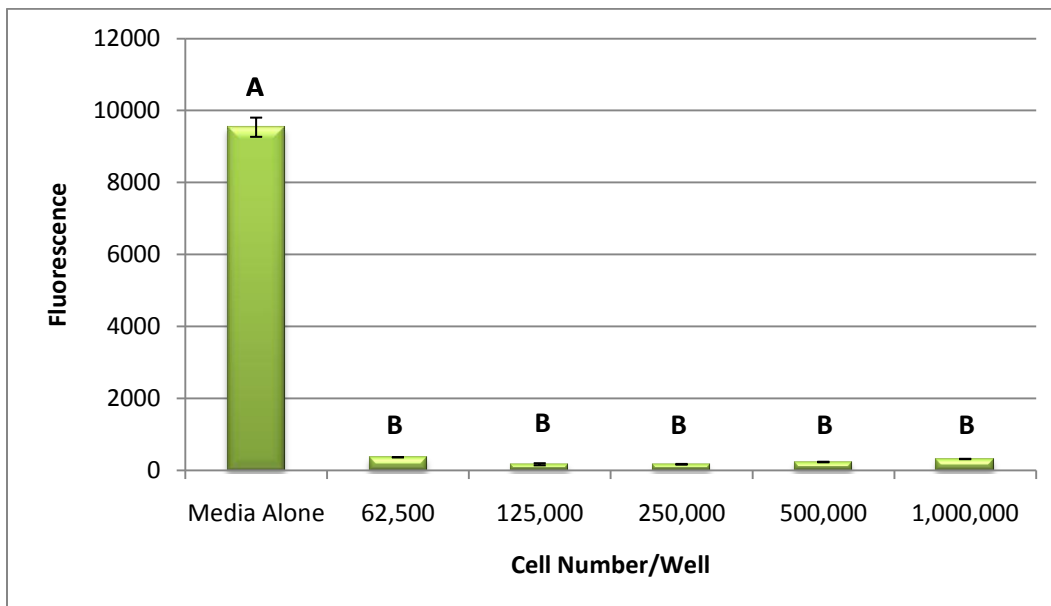
Wells +/- cells (ranging from 62,500 cells/well – 1x10^6 cells/well) were incubated for four hours in the presence of 2.5µM H$_2$0$_2$ at 37°C, in the absence of light. Extracellular H$_2$O$_2$ depletion was measured using the Amplex Red protocol. Different alphabetic letters represent statistically significant differences in fluorescent detection (p≤0.05).

3.5.2   One Hour Incubation Period

The 4 hour incubation period of the last experiment may have allowed smaller cell numbers to deplete as much hydrogen peroxide as larger cell concentrations. Therefore, the experiment was repeated using shorter incubation times. In addition, the effect of different incubation temperatures was also investigated. Using a 24 well TCP plate, RAW 264.7 cells were plated in sextuplet at different concentrations (1x10^6, 5x10^5, 2.5x10^5, 1.25x10^5, 6.25x10^4 cells/ml, as well as a control) in 1ml of complete media. The plate was placed in a 37^{0}C incubator for 6 hours, after which time the wells were washed 3 times with PBS. Subsequently, each well was filled with 500µl 2.5µM H$_2$0$_2$. Half of the wells were placed into a 37^{0}C incubator, while the other half were left to stand at room temperature (21^{0}C) for 1 hour in the absence of light. After 1 hour, the supernatant from all wells was removed and centrifuged at 13,000 rpm for 30 seconds. A 50µl sample/well was then removed near the surface of the supernatant and read for H$_2$0$_2$ using the Amplex Red protocol. Results demonstrated that incubation temperature, cell number, and

the interaction of incubation temperature and cell number all had significant effects. When specifically examining cells incubated at 37^0C, all wells containing cells depleted significantly more H_2O_2 than control. In addition, H_2O_2 depletion was found to be cell number dependent, with each cell number depleting significantly more H_2O_2 than the last (except when comparing 500,000 cells to 1,000,000 cells). This same effect was seen when the experiment was conducted at room temperature. When comparing results at different temperatures, cells incubated at room temperature depleted significantly less H_2O_2 than those incubated at 37^0C. However, this difference in depletion was not apparent between 500,000 to 1,000,000 cells (figure 17).

Figure 17: Effect of RAW 264.7 Macrophage Cell Number and Incubation Temperature on Extracellular H_2O_2 Depletion after One Hour

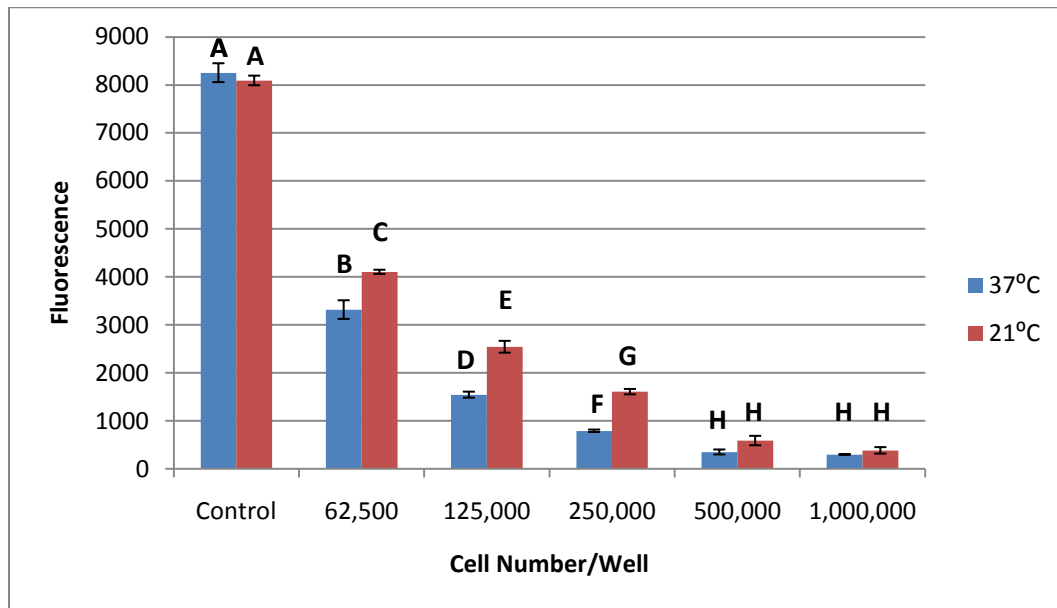Wells +/- cells (ranging from 62,500 cells/well – $1x10^6$ cells/well) were incubated for one hour in the presence of 2.5µM H_2O_2 at 21 and 37^oC, in the absence of light. Extracellular H_2O_2 depletion was measured using the Amplex Red protocol. Different alphabetic letters represent statistically significant differences in fluorescent detection ($p \leq 0.008$).

3.6 Effect of a Catalase Inhibitor on RAW 264.7 Mediated H_2O_2 Depletion

3.6.1 Effect of Catalase Inhibitor on Amplex Red Standard Curve

As catalase in one of the main mechanisms for conversion of H_2O_2 to H_2O, we investigated whether a catalase inhibitor could block RAW 264.7 cells from causing H_2O_2 depletion. A H_2O_2 standard curve, similar to ones used in prior experiments ($10\mu M – 0.08\mu M$) was created. In addition, a second standard curve was performed in which 50mM 3-amino-1,2,4-triazole (3AT, Sigma) was present. Results demonstrated a significant difference in H_2O_2 detection with 25%, 23% and 26% less fluorescence at 2.5, 5μM and 10μM H_2O_2 respectively, for Amplex Red treated with 50mM 3AT (figure 18).

Figure 18: Amplex Red Fluorescent Detection of Different Concentrations of H_2O_2 in PBS +/- 3AT
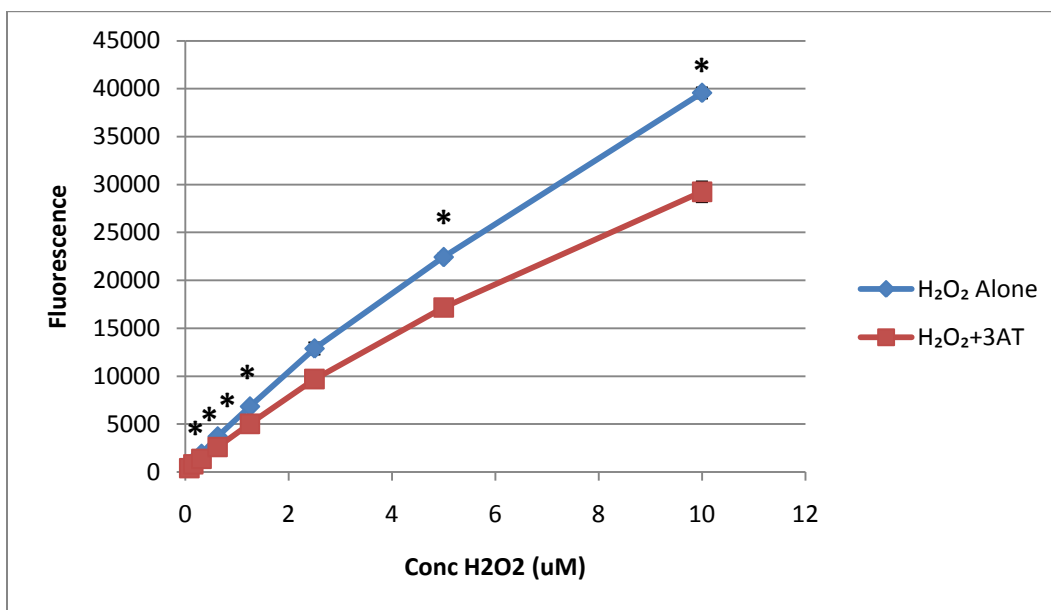
Concentrations of H_2O_2 (0.08μM to 10μM) +/- 50mM 3AT were tested using the Amplex Red protocol. All measurements performed at 21°C in the absence of light. Asterisks indicate a statistically significant difference in fluorescent detection between H_2O_2 alone versus H_2O_2+3AT at the corresponding concentration (p≤0.006).

3.6.2 Effect of 3AT on RAW 264.7 H_2O_2 Depletion

Since the previous experiment demonstrated that 50mM 3AT could negatively affect fluorescence results produced by Amplex Red, the following experiment was conducted in order

to determine how concentrations in the range 2-50mM 3AT would affect H_2O_2 depletion, by different numbers of RAW 264.7 cells. Using two 24 well TCP plates, RAW 264.7 cells were plated in 15 wells at 1×10^6 cells/ml and another 15 wells at 2.5×10^5 cells/ml in 1ml complete media. Two control groups were included: control A = 3 wells with 1ml of cells at 1×10^6 cells/ml and another 3 wells with 1ml of cells at 2.5×10^5 cells/ml in complete media (absence of inhibitor); and control B = 6 wells with 1ml complete media (3 wells for each cell concentration) (absence of inhibitor and cells). The plate was placed in a 37^0C incubator for 6 hours, after which time the samples were washed 3 times with PBS. After washing all wells, each test well was filled with a 500µl solution consisting of 2.5µM H_2O_2 and different concentrations of 3AT: 2, 5, 10, 20 and 50 mM. Control wells only received 2.5µM H_2O_2 in PBS in 500µl PBS. The plates were incubated at 37^0C for one hour, after which the supernatants were removed and centrifuged at 13,000rpm for 30 seconds. A 50µl sample was then removed from the surface of each supernatant, and tested for H_2O_2 according to the Amplex Red protocol (figure 19).

Figure 19: Protocol for Determining the Effect of 3AT on RAW 264.7 H_2O_2 Depletion
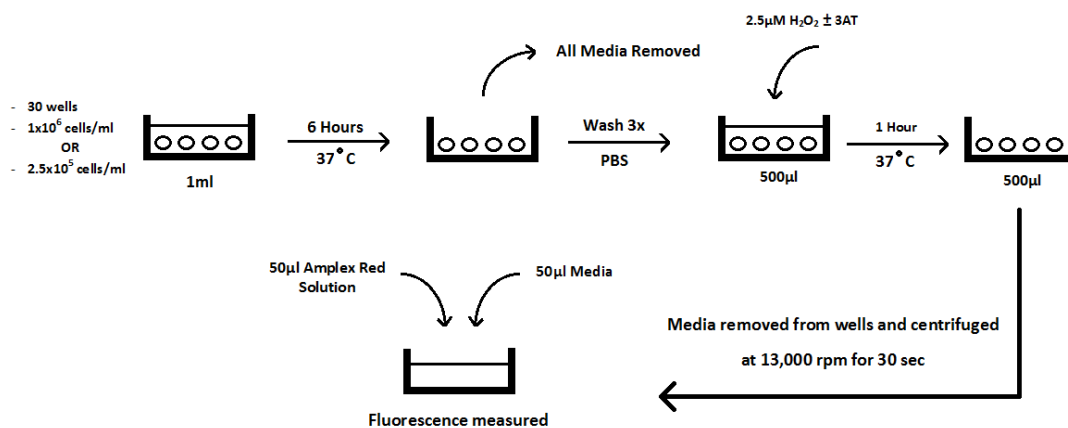
Cell number, inhibitor concentration and the interaction between cell number and inhibitor concentration all had significant effects. For 1,000,000 cells/well, one way ANOVA revealed significantly less H_2O_2 depletion for cell free controls (control B), compared to all other samples.

No differences in depletion were observed when comparing any of the remaining samples with cells. A similar trend was also observed for 250,000 cells/well, however, significantly less depletion was found for a 3AT concentration of 10,000μM over control A. When directly comparing wells with cells, all 3AT wells with 250,000 cells/well produced significantly less H_2O_2 depletion than their 1,000,000 cell/well counterpart (figure 20).

Figure 20: The Effect of Different Concentrations of Catalase Inhibitor 3AT on H_2O_2 Depletion by RAW 264.7 Macrophages
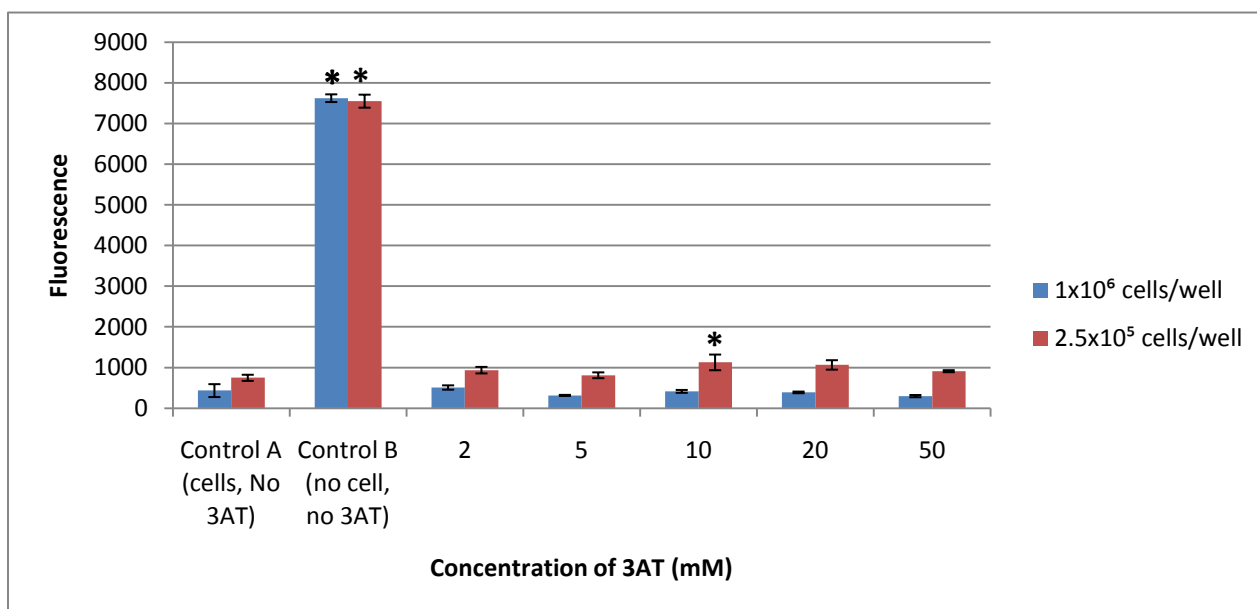
Wells with different concentration of cells were incubated for one hour with 2.5μM H_2O_2 +/- 3AT (2-50mM), at 37°C in the absence of light. All wells tested for extracellular H_2O_2 depletion using the Amplex Red protocol. Asterisks represent a statistically significant difference in fluorescent detection compared to the corresponding cell concentration in Control A (p≤0.05).

3.6.3   Effect of LPS±3AT on RAW 264.7 H_2O_2 Depletion and Amplex Red

As LPS has been demonstrated to stimulate H_2O_2 production from macrophages (Woo et al., 2004; and Park et al., 1999), the following experiment was conducted to determine whether LPS and 3AT could reverse the observed H_2O_2 depletion by RAW 264.7 cells. Using 24 well TCP plates, RAW 264.7 cells were plated in 12 wells at $1x10^6$cells/ml and 12 wells at $2.5x10^5$cells/ml concentrations, to a volume of 1ml in complete media. Twenty four additional wells served as

cell free controls, receiving only 1ml of complete media to start. The plates were placed in a 37^0C environment, and allowed to incubate for 6 hours. After 6 hours, the wells were washed 3 times with PBS. In each cell concentration category ($1x10^6$ cells/ml, $2.5x10^5$ cells/ml and cell free control), 3 wells received 500µl of: PBS alone, 1µg/ml *E.coli* LPS in PBS, 20,000µM 3AT in PBS or 1µg/ml E.coli LPS + 20,000µM 3AT in PBS. The wells incubated for 1 hour, after which time the supernatants were removed and centrifuged at 13,000 rpm for 30 seconds. A 50µl sample was removed from the surface of each supernatant, and measured for H_2O_2 using the Amplex Red protocol (figure 21).

Figure 21: Protocol for Determining of LPS±3AT on RAW 264.7 H_2O_2 Depletion and Amplex Red
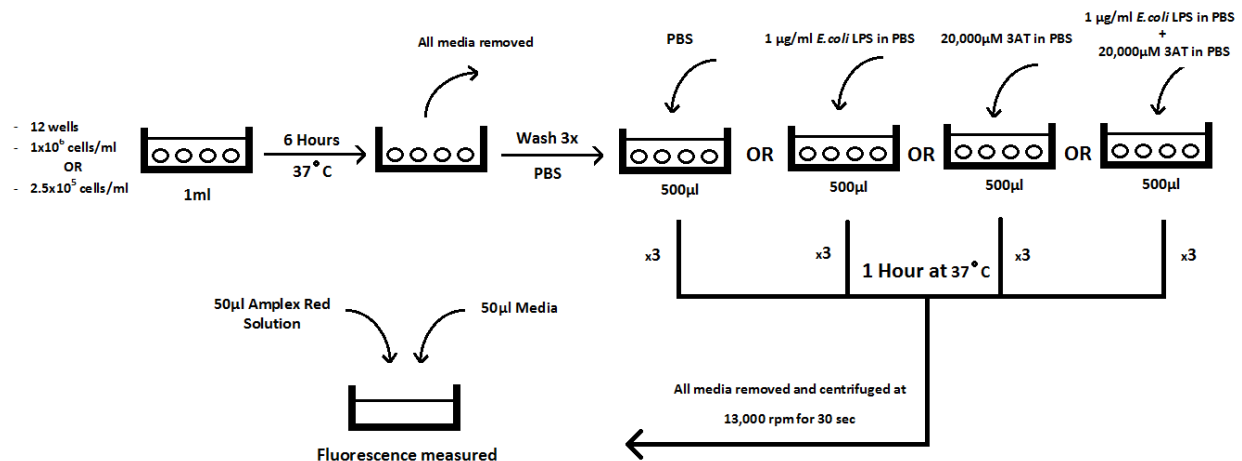
When examining the effects of LPS and 3AT on macrophage depletion of H_2O_2 neither LPS, 3AT, nor LPS+3AT were significantly different from cells with PBS alone. In addition, when directly comparing the two different cell concentrations, there was no difference in H_2O_2 depletion for any condition tested (figure 22). When examining the effects of LPS and 3AT on the Amplex Red detection reagent from cell free controls, PBS alone demonstrated significantly more fluorescence than both 3AT and LPS+3AT. There was no statistical difference between PBS alone and LPS. The only other significant difference was the greater amount of fluorescence for LPS compared to 3AT and LPS+3AT (figure 23). Therefore, catalase is not the

principal mechanism for H_2O_2 depletion observed in these experiments, and 3AT concentrations ≥20mM interfere with the detection ability of Amplex Red.

Figure 22: Effect of LPS and 3AT on RAW 264.7 Macrophage Depletion of H_2O_2
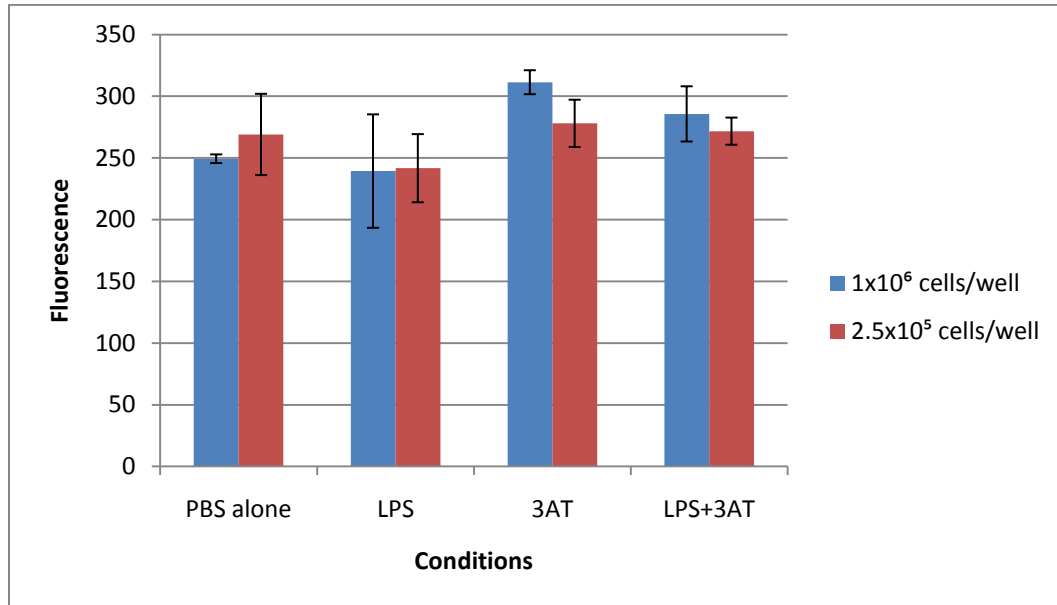
Wells with different cell concentrations were incubated ± LPS and/or 3AT for 1 hour at 37°C, in the absence of light. Extracellular H_2O_2 was tested using the Amplex Red protocol. None of the conditions tested produced statistically significant differences in fluorescent detection compared to PBS alone (p≤0.05).

Figure 23: Effect of LPS and 3AT on Amplex Red Detection Reagent
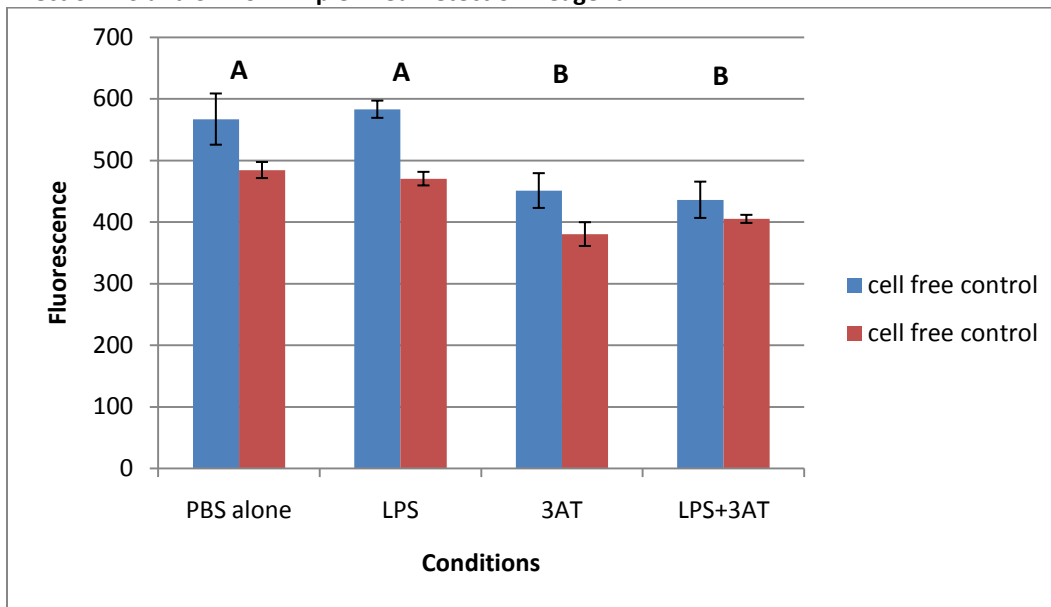
Cell free wells were incubated ± LPS and/or 3AT for 1 hour at 37°C, in the absence of light. H_2O_2 was tested using the Amplex Red protocol. Different alphabetic letters represent statistically significant differences in fluorescent detection (p≤0.05).

3.7 Effect of Number of Passages of RAW 264.7 Cells on H_2O_2 Depletion

It is possible that multiple passages of RAW 264.7 cells over time selected for certain cell characteristics, so a new stock of RAW 264.7 cells was acquired from ATCC to determine whether cells which had undergone less passaging, behaved differently than those used for all previous experimentation. Newly acquired RAW 264.7 cells (ie. NEW) were incubated in complete culture media within a 75cm^2 flask. Using a 24 well TCP plate, 1ml of both NEW and ORIGINAL RAW 264.7 cells were plated in triplicate at: $1x10^6$, $5x10^5$, $2.5x10^5$, $1.25x10^5$, $6.25x10^4$ cells/ml and control. The plate was then allowed to incubate at 37°C for 6 hours. After 6 hours, all wells were washed 3 times with PBS, and then treated with 500µl 2.5µM H_2O_2 in PBS for one hour at 37°C. Subsequently, the supernatants were removed and centrifuged at 13,000 rpm for 30 seconds. A 50µl sample was then obtained from the surface of each supernatant, and tested for the presence of H_2O_2 using the Amplex Red protocol. Two factor ANOVA demonstrated a significant effect of cell concentration, cell type (NEW vs ORIGINAL) and the combination of the two on H_2O_2 depletion outcome. More specifically, when examining

results from the ORIGINAL RAW 264.7 cell line, each cell concentration tested was found to produce significantly less H_2O_2 depletion that the next higher concentration, except when comparing 1,000,000 cells/well to 500,000 cells/well. A similar trend was observed for the NEW RAW 264.7 cell line, with no significant difference in depletion between 250,000 cells/well, 500,000 cells/well and 1,000,000 cells/well. When directly comparing ORIGINAL versus NEW cells, NEW cells were found to demonstrate significantly more H_2O_2 depletion than ORIGINAL cells, except at 1,000,000 cells/well (figure 24).

Figure 24: Effect of Passage Number on RAW 264.7 Macrophage-Mediated Depletion of Extracellular H_2O_2
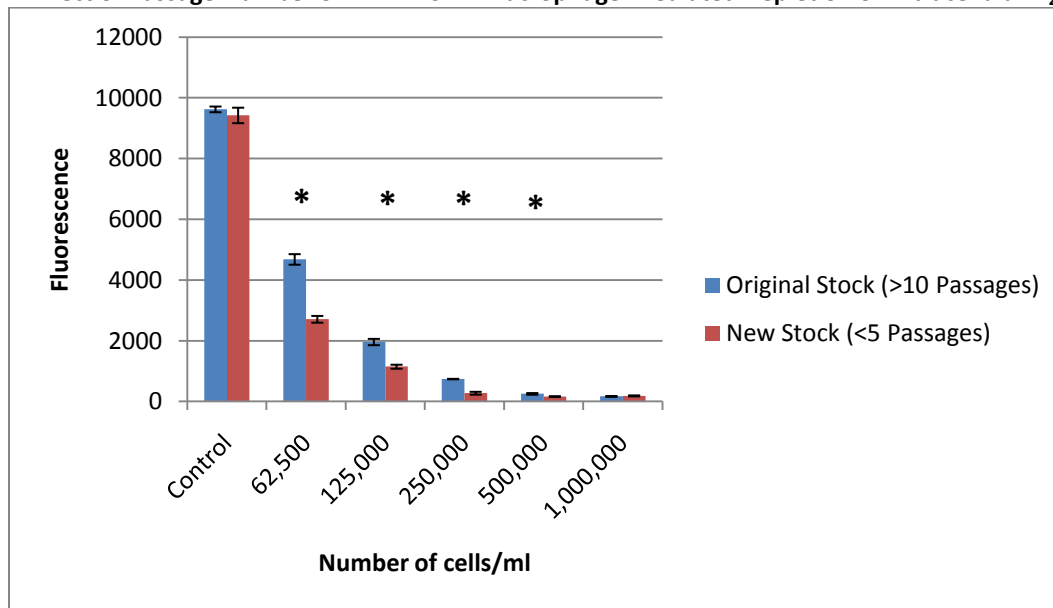
Cells with different passage numbers (<5 versus >10) were plated at different concentrations (0 – 1x10^6 cells/well) with 2.5µM H_2O_2 for 1 hour at 37°C, in the absence of light. Extracellular H_2O_2 depletion was measured using the Amplex Red protocol. Asterisks represent statistically significant difference in fluorescent detection between stocks at the corresponding cell concentration ($p \leq 0.0.008$).

4 Discussion, Conclusions and Future Directions

4.1 Discussion

The majority of studies on production of ROS from RAW 264.7 macrophages used DCFDA as the detection reagent to examine both intra and extracellular concentrations of reactive oxygen species (Kim et al., 2009; Kimura et al., 2008; and Yoo et al., 2002). In contrast, only one study (Mantena et al., 2008) used a specific agent (Amplex Red) that targeted hydrogen peroxide production from RAW 264.7 cells. The purpose of the present investigation was to examine the production and depletion of hydrogen peroxide by RAW 264.7 macrophages in tissue culture. The amount of hydrogen peroxide present was assessed via the oxidation and fluorescence of Amplex Red; a detection reagent specific to H_2O_2.

4.1.1 RAW 264.7 Macrophage-Mediated Depletion of H_2O_2

Macrophages were found to deplete significant amounts of exogenously added hydrogen peroxide. This depletion was found to be time, cell concentration, incubation temperature, and passage number dependent. In addition, the stimulating effect of LPS on extra- or intracellular H_2O_2 production could not be demonstrated. These results are in contrast to past research that demonstrated that macrophages are producers of reactive oxygen species, including hydrogen peroxide, and that LPS could stimulate H_2O_2 production (Kimura et al., 2008; Woo et al., 2004; and Park et al., 1999). The difference in results may be attributed to the use of the detection reagent DCFDA, which not only detects hydrogen peroxide, but other reactive oxygen species such as peroxynitrite, hydroxyl radicals, lipid peroxidases, nitric oxide, and hypochlorite (Rhee et al., 2010).

The lack of hydrogen peroxide stimulation with LPS is also in contrast to previous studies (Park et al., 1999; and Woo et al., 2004). This again may be due to the fact that these studies used DCFDA to "detect" H_2O_2, when in actuality; they were detecting many different reactive oxygen species that could have been stimulated by LPS.

The ability of the macrophage to deplete exogenous H_2O_2 may be attributed to one or more of its numerous antioxidant systems, which include catalase, Prx, Cu^+/Fe^{2+} and/or GPx/GSH (Benzie

2000; and Karihtala et al., 2007). Studies by Carter et al (2004) have demonstrated that the high level of catalase and GPx activity within alveolar macrophages can limit the effectiveness of H_2O_2 as a second messenger. Alternatively, the enzyme myeloperoxidase may have catalyzed a reaction which converted most of the extracellular hydrogen peroxide to a product that could not be detected by Amplex Red ($H_2O_2 + Cl^- \rightarrow HOCl$). This study demonstrated that macrophages could deplete exogenous H_2O_2 rapidly. Any cell concentration tested depleted all exogenously added H_2O_2 after 4 hours, so that even lower concentrations of cells were able to deplete the same amount of exogenous H_2O_2 at higher concentrations. The process was even efficient enough to cause significant depletion of exogenous hydrogen peroxide after only one hour of incubation.

The effect of increased temperature on H_2O_2 depletion can be explained by an increase in chemical reaction rates, which lead to greater depletion of H_2O_2 over time.

The effect of multiple culture passages, which influenced the macrophage's ability to deplete H_2O_2, has also been demonstrated by past research to effect: electrical resistance, enzyme activity, transporter function and CYP3A4 mRNA production in Caco-2 cells (Sambuy et al., 2005); decreased doubling time, increased plating efficiency, and decreased yield in the number of cells per plate for Syrian hamster embryo (SHE) cells (Chang-Liu et al., 1997); changes in response of prostatic adenocarcinoma line (LNCaP) cells to androgens and retinoic acid (Esquenet et al., 1997); and reduced protein expression of RAW 264.7 cells (Jacobson et al., 2007). The changes due to passage number can be attributed to the stresses produced on cells from being in a foreign environment. Competition for survival and repeated cell culture passaging creates selection pressures, which can lead to the development of certain cell characteristics that optimize cell survival in culture (ATCC 2007; and Sambuy et al., 2005).

The significance of these findings is that the macrophage could deplete large amounts of extracellular hydrogen peroxide recently used to fight an infection. By this depletion, an extracellular environment more suitable to the early stages of healing may be established (Roy et al., 2006), along with the elimination of intracellular signaling that trigger the release of proinflammatory cytokines (Forman et al 2010A and B; Halliwell et al., 2000; and Schreck et al

1991). An important next step is the determination of which mechanism causes the depletion of hydrogen peroxide by RAW 264.7 macrophages.

4.1.2   3AT Failed to Block H$_2$O$_2$ Depletion and Negatively Affected Amplex Red

The addition of the catalase inhibitor, 3-amino-1,2,4-triazole (3AT), was not found to inhibit the macrophage-mediated depletion of hydrogen peroxide at concentrations up to 50mM. In addition, we concluded that 3AT reduced the ability of Amplex Red to detect hydrogen peroxide. The ability of 3AT to interfere with detection reagents has not been observed in other studies that used concentrations ranging from 10mM-25mM (Keith et al., 2009; Carter et al., 2004; and Vega et al., 2004). However, none of these studies used Amplex Red as a detection reagent. A literature search performed in December 2010 did not locate any articles that simultaneously used Amplex Red and 3AT, or any which specifically investigated the effect of 3AT on RAW 264.7 cellular function. The findings from the current study indicate that an antioxidant system other than/in addition to catalase, such as Cu^+/Fe^{2+}, GSH/GPx, Prx and/or myeloperoxidase, is primarily involved in RAW 264.7 hydrogen peroxide depletion, and that the catalase inhibitor, 3AT, negatively affects the detection abilities of Amplex Red. The significance of these results is that in order to further understand macrophage H$_2$O$_2$ depletion, additional testing of possible antioxidant mechanisms is required.

4.1.3   PBS Media and Black Microplates Provide the Best Conditions for Measuring Fluorescence

Fluorescent readings in DMEM and complete media were both found to be significantly lower than readings in PBS. In addition, when measuring the same amount of hydrogen peroxide, clear microplates produced significantly more fluorescence than black walled microplates. These differences can be explained by 2 phenomena. The first is well-to-well crosstalk, in which a certain amount of light can 'leak' through the walls of a clear/white well, and are then erroneously detected in adjacent wells. The second is the auto-fluorescence of the material of the plates (polystyrene). Treating plates with 1% carbon black, thus producing a black coloured microplate, has been found to significantly reduce both autofluorescence and well-to-well crosstalk (Hidex Personal Life Science; Knight S; and Promega 2011). The significance of these

findings is that all measurements of hydrogen peroxide by Amplex Red should be conducted in PBS within a black microplate

Differences in fluorescence within different media may be attributed to inhibition by certain components in these later two media. Complete media used in the present study is made up of a number of components, including 15% fetal calf serum. Previous studies have demonstrated that the presence of serum can lead to the decomposition of H_2O_2 (Link et al., 1988), and therefore, produce less fluorescence in the presence of Amplex Red. In addition phenol red, a pH indicator found in some preparations of DMEM, has also been found to lead to significant quenching of fluorescent reactions (Pawley JB 2006; and Gilbert et al., 2000).

4.1.4   RAW 264.7 Macrophages Affect the Ability of Amplex Red to Detect H_2O_2

After being exposed to RAW 264.7 macrophages, the ability of Amplex Red to detect a known amount of exogenously added hydrogen peroxide was reduced. Similar results were demonstrated by Votyakova et al (2004), where it was determined that the HRP used in Amplex Red reactions could catalyze the oxidation of NADH and glutathione to produce additional amounts of H_2O_2, which were then detected by the reagent, thus reducing the amount of Amplex Red available for further detection. Alternatively, the macrophages may have released a substance into the media, which interfered with Amplex Red's detection capabilities. Such a reaction may have occurred via myeloperoxidase, which catalyzes the reaction of H_2O_2 and chloride ion into hypochlorous acid. The reactive hypochlorous acid produced may have reacted with Amplex Red to form a non-fluorescent product.

4.2 Conclusions

1. Amplex Red could be used to quantitatively measure amounts of H_2O_2 when PBS medium and black walled microplates were used.

2. Raw 264.7 macrophages were found to produce small, yet significant amounts of hydrogen peroxide. LPS had no discernible effect on this production.

3. The RAW 264.7 macrophage was found to deplete exogenously added hydrogen peroxide.

4. Hydrogen Peroxide depletion by RAW 264.7 cells was found to be time, cell concentration, temperature and passage number dependent.

5. The use of a catalase inhibitor, 3AT, had no effect on reducing the ability of RAW 264.7 cells to deplete hydrogen peroxide from its surrounding environment, and was also found to lower the detection capacity of Amplex Red. The depletion mechanism is unknown at present.

6. The lack of H_2O_2 detection by Amplex Red may be attributed to a substance released by the RAW 264.7 macrophage, which affects the reagent's conversion to a fluorescent product.

4.3 Future Directions

The results from the current study clearly indicate that further research is required to understand the process of RAW 264.7 macrophage-mediated depletion of hydrogen peroxide. The rationale for further study is that it will yield a better understanding as to how macrophages and hydrogen peroxide play a role in wound healing:

1. The results of previous studies that used DCFDA to detect hydrogen peroxide should be repeated using a detection reagent specific to H_2O_2, such as Amplex Red. In doing so, researchers could eliminate whether the products detected were reactive oxygen species other than hydrogen peroxide.

2. The use of different detection reagents specific to hydrogen peroxide, such as the Fox Method, TMB, deprotection-based fluorescent probes, SNAP-tag protein labeling (Rhee et al., 2010) and/or electrochemical detection (Zhang et al., 2010) could be used in order to confirm the results of the current study. In addition, if a finite amount of Amplex Red is being converted to a non-fluorescent product, additional amounts of Amplex Red could be added to the cell free supernatant, which would then be free to detect any hydrogen peroxide present.

3. Other macrophage cells lines, or freshly isolated human macrophages, could be tested in order to determine whether depletion of hydrogen peroxide is specific to RAW 264.7 cells.

4. Different inducers of hydrogen peroxide production such as phorbol myristate acetate (Hughes et al., 2006), or LPS from different bacteria, should be tested for their ability to induce hydrogen peroxide in RAW 264.7 cells.

5. In order to determine the mechanisms underlying the RAW 264.7 cells' ability to deplete H_2O_2, different antioxidant pathways could be blocked by using specific inhibitors directed against each pathway: mercaptosuccinic acid for GPx (Conde de la Rosa et al., 2006); conoidin A for peroxiredoxin (Liu et al., 2010); L-buthionine-(S,R)-sulfoximine (BSO) for GSH (Lee et al., 2008); and/or 4-Aminobenzoic acid hydrazide (ABAH) for myeloperoxidase (Kettle et al., 1997).

6. Further research on implant healing may be conducted by examining the effect of titanium implant surface topography and chemistry on the ability of the RAW 264.7 macrophage to deplete hydrogen peroxide.

References

Abbas, AK., Lichtman, AH., & Pillai, S. (2007). Cellular and Molecular Immunology. 6th Edition. Philadelphia, PA: Saunders Elsevier. pp 4, 35-37.

Abe J et al. Fyn and JAK2 Mediate Ras Activation by Reactive Oxygen Species. J Biol Chem 1999; 274: 21003-21010.

Alberts, B., et al. (2008). Molecular Biology of the Cell. 5th Edition. New York, NY: Garland Publishing. pp 618-1245.

American Type Culture Collection (ATCC) Product Description: TIB-71. (2010) Retrieved January 5, 2011from http://www.atcc.org/ATCCAdvancedCatalogSearch/productDetails/tabid/452/Default.aspx?ATCCNum=TIB-71&Template=cellBiology

American Type Culture Collection. (2007). Passage Number Effects in Cell Lines. Why They Happen and What You can do About it. Retrieved on January 5, 2011 from http://www.genengnews.com/transfection/ATCC_TechBulletin_7_Final_06_07.pdf

American Type Culture Collection (ATCC) Cell Line Index Catalog (n.d.). Retrieved January 5, 2011 from http://www.atcc.org/Portals/1/Pdf/CellCatalog/CellTissue.pdf

Bartosz G. Use of Spectroscopic Probes for Detection of Reactive Oxygen Species. Clin Chim Acta 2006; 368: 53-76.

Battin EE et al., Antioxidant Activity of Sulfur and Selenium; A Review of Reactive Oxygen Species Scavenging, Glutathione Peroxidase, and Metal-Binding Antioxidant Mechanisms. Cell Biochem Biophys 2009; 55: 1-23.

Benzie IFF. Evolution of Antioxidant Defence Mechanisms. Eur J Nutr 2000; 39: 53-61.

Bozonet SM et al. Oxidation of a eukaryotic 20Cys peroxiredoxin is a molecular switch controlling the transcriptional response to increasing levels of hydrogen peroxide. J Biol Chem 2005; 280: 23319-23327.

Cadenas E. Basic Mechanisms of Antioxidant Activity. BioFac 1997; 6: 391-397.

Campbell, NA., Reece, JB., & Mitchell LG. (1999). Biology. 5th Edition. Menlo Park, California: Benjamin/Cummings. pp 842-852.

Carter AB et al. High Levels of Catalase and Glutathione Peroxidase Activity Dampen H_2O_2 Signaling in Human Alveolar Macrophages. Am J Respir Cell Mol Biol 2004; 31: 43-53.

Chang-Liu CM et al. Effect of Passage Number on Cellular Response to DNA-damaging Agents: Cell Survival and Gene Expression. Cancer Letters 1997; 113: 77-86.

Davies JE. Understanding Peri-implant Endosseous Healing. J Dent Educ 2003; 67: 932-949.

De Nardin E. The Role of Inflammatory and Immunological Mediators in Periodontitis and Cardiovascular Disease. Ann Periodontol 2001; 6: 30-40.

Dennsion DK et al. The Acute Inflammatory Response and the Role of Phagocytic Cells in Periodontal Health and Disease. Periodontology 2000 1997; 14: 54-78.

Esquenet M et al. LNCaP Prostatic Adenocarcinoma Cells Derived from Low and High Passage Numbers Display Divergent Responses not only to Androgens but also to Retinoids. J Steroid Biochem Molec Biol 1997; 62: 391-399.

Fairweather D et al. Alternatively Activated Macrophages in Infection and Autoimmunity. J Autoimmun 2009; 33: 222-230.

Forman HJ et al A. Signaling Functions of Reactive Oxygen Species. Biochem 2010; 49: 835-842.

Forman HJ et al B. Reactive Oxygen Species and α,β-unsaturated aldehydes as second messengers in signal transduction. Ann NY Acad Sci 2010; 1203: 35-44.

Gay C et al. A Critical Evaluation of the Effect of Sorbitol on the Ferric-Xylenol Orange Hydroperoxide Assay. Anal Biochem 2000; 284: 217-220.

Gilbert PA et al. On-Line Measurement of Green Fluorescent Protein (GFP) Fluorescence for the Monitoring of Recombinant Adenovirus Production. Biotechnology Letters 2000; 22: 561-567.

Haddad JJ. Antioxidant and Prooxidant Mechanisms in the Regulation of Redox(y)-Sensitive Transcription Factors. Cellular Signalling 2002; 14: 879-897.

Halliwell B. Antioxidant Defence Mechanisms: From the Beginning to the End (of the Beginning). Free Rad Res 1999; 31: 261-272.

Halliwell B et al. Hydrogen Peroxide in the Human Body. FEBS Letters 2000; 486: 10-13.

Hanukoglu I. Antioxidant Protective Mechanisms Against Reactive Oxygen Species (ROS) Generated by Mitochondral P450 Systems in Steroidogenic Cells. Drug Meta Rev 2006; 38: 171-196.

Hartley JW et al. Expression of Infectious Murine Leukemia Viruses by RAW 264.7 Cells, a Potential Complication for Studies with a Widely Used Mouse Macrophage Cell Line. Retrovirology 2008; 5: 1-6.

Hidex Personal Life Science: Plate Chameleon Technical Note. (n.d.). Doc 512-004; Version 1.0. Accessed January 9, 2011 from http://www.interactivebioscience.cz/admin/_docs/protokol%20-%20Crosstalk.pdf

Hunt JA et al. Effect of Biomaterial Surface Charge on the Inflammatory Response: Evaluation of Cellular Infiltration and TNFα Production. J Biomed Mater Res 1996; 31: 139-144.

Jacobson L et al. Effects of Passage Number on Cell Line Transfection. Biochemica 2007; 3.

Karihtala P et al., Reactive Oxygen Species and Antioxidant Mechanisms in Human Tissues and their Reaction to Malignancies. APMIS 2007; 115: 81-103.

Keith KE et al. Delayed Association of the NADPH Oxidase Complex with Macrophage Vacuoles Containing the Opportunistic Pathogen *Burkholderia cenocepacia*. Microbiology 2009; 155: 1004-1015.

Kettle AJ et al. Mechanism of Inactivation of Myeloperroxidase by 4-Aminobenzoic Acid Hydrazide. Biochem J 1997; 321 (pt 2): 503-508.

Kim D et al. 2,4-Dinitrofluorobenzene Modifies Cellular Proteins and Induces Macrophage Inflammatory Protein-2 Gene Expression via Reactive Oxygen Species Production in RAW 264.7 cells. Immuno Inves 2009; 38: 132-152.

Kimura k et al. Inhibition of Reactive Oxygen Species Down-Regulates Protein Synthesis in RAW 264.7. Biochem Biophys Res Comm 2008; 372: 272-275

Knight S. (n.d.). Laboratory News Online: Picking the Perfect Plate. Accessed January 9, 2011 from http://www.labnews.co.uk/printer_friendly.php/5633/picking-the-perfect-plate

Kumar, V., Cotran, RS., & Robbins SL. (2003). Robbins Basic Pathology. 7th Edition. Philadelphia, PA: Saunders. Pp 1-55.

Link EM et al. Role of Hydrogen Peroxide in the Cytotoxicity of the Xanthine/Xanthine Oxidase System. Biochem J 1988; 249: 391-399.

Maeda H et al. A Design of Fluorescent Probes for Superoxide Based on a Nonredox Mechanism. J Am Chem Soc 2005; 127: 68-69.

Mantena RK et al. Reactive Oxygen Species are the Major Antibacterials Against *Salmonella* Typhimurium Purine Auxotrophs in the Phagosome of RAW 264.7 Cells. Cell Micro 2008; 10: 1058-1073

Masella R et al., Novel Mechanisms of Natural Antioxidant Compounds in Biological Systems: Involvement of Glutathione and Glutathione-related Enzymes. J Nutr Biochem 2005; 16: 577-586.

Meyer M et al. H_2O_2 and Antioxidants have Opposite Effects on Activation of NF-κB and AP-1 in Intact cells: AP-1 as Secondary Antioxidant-Responsive Factor. The EMBO journal 1993; 12: 2005-2015.

Miller EW et al. Molecular Imaging of Hydrogen Peroxide Produced for Cell Signalling. Nat Chem Biol 2007; 3: 263-267.

Mohanty JG et al. A Highly Sensitive Fluorescent Micro-Assay of H_2O_2 Release from Activated Human Leukocytes using a Dihydroxyphenoxazine Derivative. J Immuno Meth 1997; 202: 133-141.

Park SY et al. Potentiation of Hydrogen Peroxide, Nitric Oxide, and Cytokine Production in RAW 264.7 Macrophage Cells Exposed to Human and Commercial Isolates of *Bifidobacterium.* Int J Food Micro 1999; 46: 231-241.

Pawley JB. (2006). Handbook of Biological Confocal Microscopy. 3rd Edition. New York, NY: Springer Science and Business Media. pp 361.

Perron NR et al., A Review of the Antioxidant Mechanisms of Polyphenol Compounds Related to Iron Binding. Cell Biochem Biophys 2009; 53: 75-100.

Polimeni G et al. Biology and Principles of Periodontal Wound Healing/Regeneration. Perio 2000 2006; 41: 30-47.

Promega. (2011). Which Plates to Choose for Fluorescence and Luminescence Measurements? Accessed on January 9, 2011 from http://www.promega.com/pubs/faq_009.htm

Raschke WC et al. Functional Macrophage Cell Lines Transformed by Abelson Leukemia Virus. Cell 1978; 15: 261-267.

Rhee S G. Redox Signaling: Hydrogen Peroxide as Intracellular Messenger. Exp and Mole Med 1999; 31: 53-59.

Rhee SG et al. Methods for Detection and Measurement of Hydrogen Peroxide Inside and Outside of Cells. Mol. Cells 2010; 29: 539-549.

Robbins, SL., Cotran, RS., & Kumar, VK. (2003). Robbins Basic Pathology. 7th Edition. Philadelphia, Penn: Sauders. pp 52-107.

Roy S et al. Dermal Wound Healing is Subject to Redox Control. Molecular Therapy 2006; 13 (1): 211-220.

Sablina et al. The Antioxidant Function of the p53 Tumor Suppressor. Nat Med 2005; 11: 1306-1313.

Sambuy Y et al. The Caco-2 Cell Line as a Model of the Intestinal Barrier: Influence of Cell Culture-Related Factors on Caco-2 Cell Functional Characteristics. Cell Bio and Toxi 2005; 21: 1-26.

Schreck R et al. Reactive Oxygen Intermediates as Apparently Widely used Messengers in the Activation of the NF-κB Transcription Factor and HIV-1. The EMBO Journal 1991; 10 (8): 2247-2258.

Sennerby L et al. Early Tissue Response to Titanium Implants Inserted in Rabbit Cortical Bone. Part II Ultrastructural observations. J Mater Sci: Mater Med 1994; 4: 494-502.

Slaets E et al. Early Cellular Responses in Cortical Bone Healing Around Unloaded Titanium Implants: an animal study. J Perio 2006; 77: 1015-1024.

Southerland JH et al. Commonality in Chronic Inflammatory Diseases: Periodontitis, Diabetes, and Coronary Artery Disease. Periodontology 2000 2006; 40: 130-143.

Srikun D et al. Organelle-Targetable Fluorescent Probes for Imaging Hydrogen Peroxide in Living Cells via SNAP-Tag Protein Labeling. J Am Chem Soc 2010; 132: 4455-4465.

Sun Yi et al. Redox regulation of Transcriptional Activators. Free Radical Biology & Medicine 1996; 21: 335-348.

Thomsen P et al. Macrophage Interactions with Modified Material Surfaces. Cur Opin Solid State Mater 2001; 5: 163-176.

Van Dyke TE. Control of Inflammation and Periodontitis. Periodontology 2000 2007; 45: 158-166.

Vander, A., Sherman, J., & Luciano, D. (2001). Human Physiology: The Mechanisms of Body Function. 8th Edition. New York, NY: McGraw-Hill. pp 1-715.

Veal EA et al., Hydrogen Peroxide Sensing and Signaling. Mole Cell Rev 2007; 26: 1-14.

Vega A et al. A New Role for Monoamine Oxidases in the Modulation of Macrophage-Inducible Nitric Oxide Synthase Gene Expression. J Leuko Bio 2004; 75: 1093-1101.

Votyakova TV et al. Detection of Hydrogen Peroxide with Amplex Red: Interference by NADH and Reduced Glutathione Auto-oxidation. Arch Biochem Biophys 2004; 431: 138-144.

Watkins SA et al. When Wound Healing Goes Awry. A Review of Normal and Abnormal Wound Healing, Scar Pathology and Therapeutics. J Drugs Derm 2008; 7(10): 997-1005.

Wikesjo ULF et al. Periodontal Wound Healing and Regeneration. Perio 2000 1999; 19: 21-39.

Witte MB et al. General Principles of Wound Healing. Surg Clin North Amer 1997; 77: 509-528.

Woo CH et al. Lipopolysaccharide Induces Matrix Metalloproteinase-9 Expression via a Mitochondrial Reactive Oxygen Species-p38 Kinase-Activator Protein-1 Pathway in Raw 264.7 Cells. J Immunol 2004; 173: 6973-6980.

Yoo HG et al. IL-1β Induces MMP-9 via Reactive Oxygen Species and NF-κB in Murine Macrophage RAW 264.7 Cells. Biochem Biophys Res Comm 2002; 298: 251-256.

Zhang LC et al. Electrochemical Detection of Extracellular Hydrogen Peroxide Released from RAW 264.7 Murine Macrophage Cells Based on Horseradish Peroxidase-Hydroxyapatitie Nanohybrids. Analyst 2010: ahead of print. Accessed on February 16, 2011 from http://www.ncbi.nlm.nih.gov/pubmed/21170446.

Zhou M et al. A Stable Nonfluorescent Derivative of Resorufin for the Fluorometric Determination of Trace Hydrogen Peroxide: Applications in Detecting the Activity of Phagocyte NADPH Oxidase and other Oxidases. Anal Biochem 1997; 253: 162-168.

Appendices

Appendix A: ANOVA tables

Determination of Optimal Conditions for Experimentation

Two Factor ANOVA: Black Microplate Alone

Source	Type III Sum of Squares	df	Mean Square	F	Sig.
Corrected Model	8.974E+09	23	3.902E+08	15413.653	0.000
Intercept	2.047E+09	1	2.047E+09	80865.266	0.000
Concentration (conc)	2.195E+09	7	3.136E+08	12390.096	0.000
Medium	3.125E+09	2	1.562E+09	61726.438	0.000
Medium*conc	3.653E+09	14	2.610E+08	10309.319	0.000
Error	1.215E+06	48	2.531E+04		
Total	1.102E+10	72			
Corrected total	8.975E+09	71			

Two Factor ANOVA: Clear Microplate Alone

Source	Type III Sum of Squares	df	Mean Square	F	Sig.
Corrected Model	1.271E+10	23	5.527E+08	5184.618	0.000
Intercept	3.503E+09	1	3.503E+09	32865.318	0.000
Concentration (conc)	3.341E+09	7	4.773E+08	4477.861	0.000
Medium	4.360E+09	2	2.180E+09	20450.781	0.000
Medium*conc	5.010E+09	14	3.579E+08	3357.116	0.000
Error	5.117E+06	48	1.066E+05		
Total	1.622E+10	72			
Corrected total	1.272E+10	71			

Two Factor ANOVA: Comparison of Black versus Clear Microplate

Source	Type III Sum of Squares	df	Mean Square	F	Sig.
Corrected Model	1.427E+10	15	9.514E+08	4828.961	0.000
Intercept	1.276E+10	1	1.276E+10	64770.149	0.000
Concentration (conc)	1.322E+08	1	1.322E+08	671.181	0.000
Medium	1.400E+10	7	2.000E+09	10152.749	0.000
Medium*conc	1.367E+08	7	1.953E+07	99.142	0.000
Error	6.304E+06	32	1.970E+05		
Total	2.807E+10	48			
Corrected total	1.428E+10	47			

Effect of LPS on RAW 264.7 Mediated H_2O_2 Production

Two Factor ANOVA: Effect of presence/absence of cells

Source	Type III Sum of Squares	df	Mean Square	F	Sig.
Corrected Model	2.450E+06	5	4.900E+05	135.459	0.000
Intercept	7.699E+06	1	7.699E+06	2128.495	0.000
Time	7.465E+04	2	3.732E+04	10.319	0.001
Cells	2.093E+06	1	2.093E+06	578.584	0.000
Time*Cells	2.824E+05	2	1.412E+05	39.037	0.000
Error	6.511E+04	18	3.617E+03		
Total	1.021E+07	24			
Corrected total	2.515E+06	23			

Two Factor ANOVA: Effect of presence/absence of LPS

Source	Type III Sum of Squares	df	Mean Square	F	Sig.
Corrected Model	4.765E+04	5	9.529E+03	6.473	0.001
Intercept	1.509E+06	1	1.509E+06	1025.087	0.000
Time	2.523E+04	2	1.262E+04	8.57	0.002
Cells	9.923E+03	1	9.923E+03	6.741	0.018
Time*Cells	1.249E+04	2	6.247E+03	4.244	0.031
Error	2.650E+04	18	1.472E+03		
Total	1.583E+06	24			
Corrected total	7.414E+04	23			

Two Factor ANOVA: Effect of location and LPS

Source	Type III Sum of Squares	df	Mean Square	F	Sig.
Corrected Model	6.937E+03	3	2.312E+03	0.347	0.792
Intercept	7.478E+05	1	7.478E+05	112.253	0.000
Location	2.326E+02	1	2.326E+02	0.035	0.855
LPS (+/-)	6.440E+03	1	6.440E+03	0.967	0.345
Location*LPS (+/-)	2.641E+02	1	2.641E+02	0.04	0.846
Error	7.994E+04	12	6.662E+03		
Total	8.347E+05	16			
Corrected total	8.688E+04	15			

One Way ANOVA: Effect of location and LPS

	Sum of Squares	df	Mean Square	F	Sig.
Between Groups	7.66E+05	4	191518.075	35.854	0.000
Within Groups	80125.5	15	5341.633		
Total	8.46E+05	19			

Effect of RAW 264.7 Cell Concentration on H_2O_2 Depletion

One Way ANOVA: 1 hour incubation

	Sum of Squares	df	Mean Square	F	Sig.
Between Groups	2.16E+08	5	43100117.47	3562.517	0.000
Within Groups	145178.667	12	12098.222		
Total	2.16E+08	17			

Two Way ANOVA: 1 hour incubation

Source	Type III Sum of Squares	df	Mean Square	F	Sig.
Corrected Model	4.949E+07	9	5.499E+06	692.263	0.000
Intercept	7.236E+07	1	7.236E+07	9109.548	0.000
Temperature	2.563E+06	1	2.563E+06	322.608	0.000
Concentration	4.598E+07	4	1.149E+07	1446.995	0.000
Temp*Conc	9.515E+05	4	2.379E+05	29.946	0.000
Error	1.589E+05	20	7.943E+03		
Total	1.220E+08	30			
Corrected total	4.965E+07	29			

One Way ANOVA: 1 hour incubation (incubated cells)

	Sum of Squares	df	Mean Square	F	Sig.
Between Groups	1.41E+08	5	28217746.62	2022.294	0.000
Within Groups	167440	12	13953.333		
Total	1.41E+08	17			

One Way ANOVA: 1 hour incubation (RT cells)

	Sum of Squares	df	Mean Square	F	Sig.
Between Groups	1.26E+08	5	25123859.52	3392.875	0.000
Within Groups	88858.667	12	7404.889		
Total	1.26E+08	17			

Effect of a Catalase Inhibitor on RAW 264.7 Mediated H₂O₂ Depletion

Two Way ANOVA: Effect of 3AT on Standard Curve

Source	Type III Sum of Squares	df	Mean Square	F	Sig.
Corrected Model	6.108E+09	16	3.817E+08	119.613	0.000
Intercept	1.561E+09	1	1.561E+09	489.229	0.000
Concentration	5.491E+09	7	7.845E+08	245.815	0.000
3AT	6.896E+07	2	3.448E+07	10.804	0.000
Conc*3AT	8.797E+07	7	1.257E+07	3.938	0.003
Error	9.893E+07	31	3.191E+06		
Total	1.074E+10	48			
Corrected total	6.207E+09	47			

Two Way ANOVA: Effect of 3AT

Source	Type III Sum of Squares	df	Mean Square	F	Sig.
Corrected Model	2.841E+06	9	3.156E+05	46.324	0.000
Intercept	1.381E+07	1	1.381E+07	2026.408	0.000
Temperature	2.563E+06	1	2.563E+06	376.109	0.000
Concentration	1.906E+05	4	4.764E+04	6.992	0.001
Temp*Conc	8.750E+04	4	2.187E+04	3.211	0.034
Error	1.363E+05	20	6.813E+03		
Total	1.678E+07	30			
Corrected total	2.977E+06	29			

One Way ANOVA: 1,000,000 cells

	Sum of Squares	df	Mean Square	F	Sig.
Between Groups	1.34E+08	6	22404646.83	3971.08	0.000
Within Groups	78987.333	14	5641.952		
Total	1.35E+08	20			

One Way ANOVA: 250,000 cells

	Sum of Squares	df	Mean Square	F	Sig.
Between Groups	1.13E+08	6	18805593.27	1399.786	0.000
Within Groups	188084.667	14	13434.619		
Total	1.13E+08	20			

Two Way ANOVA: Effect of LPS±3AT on macrophages

Source	Type III Sum of Squares	df	Mean Square	F	Sig.
Corrected Model	1.250E+04	7	1.786E+03	2.827	0.040
Intercept	1.727E+06	1	1.727E+06	2733.666	0.000
Concentration	2.407E+02	1	2.407E+02	0.381	0.546
Condition	9.954E+03	3	3.318E+03	5.252	0.010
Conc*condition	2.308E+03	3	7.694E+02	1.218	0.335
Error	1.011E+04	16	6.318E+02		
Total	1.750E+06	24			
Corrected total	2.261E+04	23			

Two Way ANOVA: Effect of LPS±3AT on Amplex Red

Source	Type III Sum of Squares	df	Mean Square	F	Sig.
Corrected Model	1.084E+05	7	1.548E+04	28.834	0.000
Intercept	5.350E+06	1	5.350E+06	9962.101	0.000
Concentration	3.308E+04	1	3.308E+04	61.598	0.000
Condition	7.017E+04	3	2.339E+04	43.554	0.000
Conc*condition	5.145E+03	3	1.715E+03	3.194	0.052
Error	8.592E+03	16	5.370E+02		
Total	5.467E+06	24			
Corrected total	1.170E+05	23			

Effect of Passage Age of RAW 264.7 Cells on H_2O_2 Depletion

Two Way ANOVA: NEW versus ORIGINAL

Source	Type III Sum of Squares	df	Mean Square	F	Sig.
Corrected Model	6.027E+07	9	6.696E+06	1096.977	0.000
Intercept	4.538E+07	1	4.538E+07	7433.879	0.000
Concentration	5.311E+07	4	1.328E+07	2174.952	0.000
Cell Type	3.307E+06	1	3.307E+06	541.8	0.000
Conc*Cell Type	3.853E+06	4	9.632E+05	157.795	0.000
Error	1.221E+05	20	6.104E+03		
Total	1.058E+08	30			
Corrected total	6.039E+07	29			

One Way ANOVA: NEW

	Sum of Squares	df	Mean Square	F	Sig.
Between Groups	1.96E+08	5	39208275.83	2799.236	0.000
Within Groups	168081.333	12	14006.778		
Total	1.96E+08	17			

One Way ANOVA: ORIGINAL

	Sum of Squares	df	Mean Square	F	Sig.
Between Groups	2.05E+08	5	41016147.92	4851.462	0.000
Within Groups	101452.667	12	8454.389		
Total	2.05E+08	17			

Appendix B: Copyright Permission

Figure 1: Reprinted from Periodontology 2000, 41, Polimeni G et al, Biology and Prinicples of Periodontal Wound Healing/Regeneration, pg 31, Copyright 2006, with permission from John Wiley and Sons.

Figure 2: Reprinted from Surgical Clinics of North America, 77, Witte MB et al, General Principles of Wound Healing, pg 512, Copyright 1997, with permission from Elsevier.

Figures 4: With kind permission from Springer Science+Business Media: Molecules and Cells, Methods for Detection and Measurements of Hydrogen Peroxide Inside and Outside of Cells, 29, 2010, pg 540, Rhee SG et al, figure number 1.

Figure 5: Reprinted from Journal of Immunological Methods, 202, Mohanty et al, A Highly Sensitive Fluorescent Micro-Assay of H_2O_2 Release from Activated Human Leukocytes using a Dihydroxyphenoxazine Derivative, pg 139, Copyright 1997, with permission from Elsevier.

Figure 6: With kind permission from Springer Science+Business Media: Molecules and Cells, Methods for Detection and Measurements of Hydrogen Peroxide Inside and Outside of Cells, 29, 2010, pg 540, Rhee SG et al, figure number 2.

Figure 7: With kind permission from Springer Science+Business Media: Molecules and Cells, Methods for Detection and Measurements of Hydrogen Peroxide Inside and Outside of Cells, 29, 2010, pg 544, Rhee SG et al, figure number 6.

Figure 8: With kind permission from Springer Science+Business Media: Molecules and Cells, Methods for Detection and Measurements of Hydrogen Peroxide Inside and Outside of Cells, 29, 2010, pg 545, Rhee SG et al, figure number 7.